NASA Technical Memorandum 87732

NASA-TM-87732 19860020877

DEVELOPMENT OF AN ALGORITHM TO MODEL AN AIRCRAFT EQUIPPED WITH A GENERIC CDTI DISPLAY

WADE C. DRISCOLL AND JACOB A. HOUCK

JULY 1986

National Aeronautics and
Space Administration

Langley Research Center
Hampton, Virginia 23665

ABSTRACT

A model of human pilot performance of a tracking task using a generic Cockpit Display of Traffic Information (CDTI) display is developed from experimental data. The tracking task is to use CDTI in tracking a leading aircraft at a nominal separation of three nautical miles over a prescribed trajectory in space. The analysis of the data resulting from a factorial design of experiments reveals that the tracking task performance depends on the pilot and his experience at performing the task. Performance was not strongly affected by the type of control system used (velocity vector control wheel steering versus 3D automatic flight path guidance and control). The model that is developed and verified results in state trajectories whose difference from the experimental state trajectories is small compared to the variation due to the pilot and experience factors.

INTRODUCTION

The Advanced Transport Operating Systems (ATOPS) program (formerly called the Terminal Configured Vehicle (TCV) program, ref. 1) has been established by NASA to perform flight management and operating systems research broadly aimed at improving the safety and efficiency of transport aircraft all-weather operations in the evolving National Airspace System. The goal of the ATOPS program is to blend recent and emerging technology advancements in airborne avionics systems and information displays with human factors into effective system concepts that can be uniformly applied to transport aircraft operating in a 1990's air traffic environment. Specific objectives of the ATOPS program are to propose and investigate concepts offering improvements to aircraft systems, flight deck design, and crew procedures providing more efficient operations; to develop and investigate ways to improve the exchange of information between aircraft and air traffic control (ATC) throughout the flight profile; and to identify and promote consideration of aircraft capabilities and limitations in the design of ATC system improvements to facilitate more efficient operations. These are accomplished by conducting analysis, simulation, and flight tests and by sponsoring similar research by the aircraft industry.

A major research facility available to the ATOPS program is the Mission Oriented Terminal Area Simulation (MOTAS) facility (ref. 2). This facility is designed to provide a highly realistic environment in which air transport crews and air traffic controllers can participate in the conduct of flight management and flight operations research studies. The goal of the study described in this report was to develop an algorithm which could be used in the Mission Oriented Terminal Area Mathematical Model (MOTAM) to model an

aircraft equipped with a generic CDTI display. This class of aircraft would be included with area navigation (RNAV), VOR/DME, MLS, ILS, etc. equipped aircraft in the model.

One type of CDTI display would enable a pilot to observe the locations of nearby aircraft on a map display in the cockpit. This information is useful when the visibility is poor and the aircraft is flying under instrument flight rules (IFR). Under IFR, the ground controller gives directions to the pilot which ordinarily keep the aircraft a safe distance from others in the area. As an added precaution, the minimal allowable separations between aircraft are increased under IFR. Unfortunately, this increases the minimum time required between successive aircraft landings and thus tends to result in a lower airport throughput rate. Thus the inability to see aircraft under IFR can result in slower landing service to incoming aircraft. CDTI enables a pilot to observe the locations of nearby aircraft, resulting in the possibility of using a modification of IFR rules for aircraft having CDTI capability. This could result in faster landing service in bad weather. In addition, CDTI offers some possible advantages regarding air traffic safety and collision avoidance when the visibility is good and the aircraft is flying under visual flight rules (VFR). Under VFR, the CDTI would allow the pilot to see the locations of aircraft not normally visible through the windscreen of the cockpit due to range or position conditions.

Some changes in the air traffic control rules will be required to realize the potential benefits from CDTI. One of the difficulties of designing a new air traffic control system is the problem of predicting performance under the new system. It is of course economically infeasible to engage a fleet of aircraft and an airport for weeks or months to study a new system. Simulation

has evolved as a primary means of evaluating system performance. The Terminal Area Air Traffic Model (TAATM) was developed to model the flow of air traffic in the vicinity of an airport terminal area. The model simulates air traffic flow by the generation of information describing the flight of aircraft arrivals and departures. In past studies, it has included terminal geometry corresponding to either of two airports (Atlanta or Denver) and has been used to study various aspects of ATC system performance.

An additional degree of modeling and realism was obtained by interfacing human pilots in a simulator cockpit with the TAATM model (refs. 3 and 4). This became the prototype for the concept of the Mission Oriented Terminal Area Simulation which allows for human pilots flying simulator cockpits to be substituted for computer-generated aircraft in the terminal area model. The result is a model of the terminal area environment (ref. 5) with human pilots and air traffic controllers interacting with simulated pilots and controllers to simulate air traffic flow. This simulation requires the use of models of human pilot and controller performance of various tasks.

A series of experiments requiring human pilots to use a generic CDTI display in tracking a leading aircraft were performed. One of the objectives of the experiments was to log data that could be used to identify parameters in a model describing human performance of the tracking task. The model may then be applied in a MOTAS-type of simulation involving human pilots in simulator cockpits interacting with each other and the models of CDTI-equipped aircraft assigned tracking tasks.

SYMBOLS

A_{edj}	experimental average separation between lead aircraft and pilot's aircraft for jth region, nmi
A_{evj}	experimental average groundspeed of the pilot's aircraft for jth region, kts
A_{mdj}	modeled average separation between lead aircraft and pilot's aircraft for jth region, nmi
A_{mvj}	modeled average groundspeed of the pilot's aircraft for jth region, kts
E_p	time integral of the squared position error between the experimental and model trajectories
E_v	time integral of the squared velocity error between the experimental and model trajectories
E	weighted sum ($W_pE_p + W_vE_v$) of position and velocity errors
H	nominal separation between the lead aircraft and the pilot's aircraft, nmi
M( ), S( )	denotes an operator which yields a sample mean and sample standard deviation, repectively
P	a vector of model parameters where the parameters are ζ, ω, H, τ
R_{edj}	experimental RMS deviation of the separation between the lead aircraft and the pilot's aircraft for the jth region
R_{evj}	experimental RMS deviation of the groundspeed for the pilot's aircraft for the jth region
R_{mdj}	modeled RMS deviation of the separation between the lead aircraft and the pilot's aircraft for the jth region
R_{mvj}	modeled RMS deviation of the groundspeed for the pilot's aircraft for the jth region
W	vector of weights applied to E_p and E_v. $W = (W_p, W_v)$, where $0 \leq W_p \leq 1$ and $W_p + W_v = 1$
X	separation error, $X = (Z_0 + H) - Z_1$, nmi

$\dot{X}$	velocity difference ($\dot{Z}_0 - \dot{Z}_1$), nmi/sec
$X_e(t)$, $\dot{X}_e(t)$	state variables at time t from an experimental run
$X_m(t;\zeta,\omega,H,\tau)$ and $\dot{X}_m(t;\zeta,\omega,H,\tau)$	state variables at time t from a model with parameters ζ, ω, H, τ
Z_0	distance from origin to the pilot's aircraft, nmi
$\dot{Z}_0$, $\ddot{Z}_0$	velocity and acceleration of pilot's aircraft, respectively, nmi/sec, nmi/sec^2
Z_1	distance from origin to lead aircraft, nmi
$\dot{Z}_1$, $\ddot{Z}_1$	velocity and acceleration of lead aircraft, respectively, nmi/sec, nmi/sec^2
ζ, ω	parameters in differential equation model
τ	delay in feeding back position and velocity errors, sec
superscripts	
T, -1	transpose and inverse, respectively

ACRONYMS

AGCS	Advanced Guidance and Control System
ATC	Air Traffic Control
ATOPS	Advanced Transport Operating Systems
CDTI	Cockpit Display of Traffic Information
CRT	Cathode Ray Tube
DME	Distance Measuring Equipment
EADI	Electronic Attitude Director Indicator
EHSI	Electronic Horizontal Situation Indicator
IFR	Instrument Flight Rules
ILS	Instrument Landing System
MLS	Microwave Landing System
MOTAM	Mission Oriented Terminal Area Model
MOTAS	Mission Oriented Terminal Area Simulation
NCDU	Navigation Control and Display Unit
RMS	Root Mean Square
RNAV	Area Navigation
TAATM	Terminal Area Air Traffic Model
TCV	Terminal Configured Vehicle
TSRV	Transport Systems Research Vehicle
VCWS	Velocity Vector Control Wheel Steering
VFR	Visual Flight Rules
VHF	Very High Frequency
VOR	VHF Omnidirectional Range
3D	3-dimensional

MOTAS FACILITY DESCRIPTION

MOTAS is a flexible, comprehensive simulation of the airborne, ground-based, and communications aspects of the terminal area environment. The major elements of MOTAS (fig. 1) are: a terminal area environment model, aircraft simulator cockpits, pseudo pilot stations, air traffic controller stations, and a realistic air-ground communications network. The terminal area environment model (ref. 5) represents today's Denver Stapleton International Airport and surrounding area using either an automated metering and spacing system of control or a manual vectoring system of control. In addition, the model simulates various radar systems, navigational aids, wind conditions, and so forth.

The facility is configured to tie-in a number of aircraft simulator cockpits including the Transport Systems Research Vehicle (TSRV) Simulator, the DC-9 Full Workload Simulator, the Advanced Concepts Simulator, and the General Aviation Simulator. This allows for a number of different types of aircraft to be flown in a realistic environment by human crews. The pseudo pilot stations (fig. 2) are devices which allow an operator to control and fly a number of computer-generated aircraft in the terminal area environment along with the aircraft simulator cockpits, thus providing the realism of the traffic density which would occur in the real world. The pseudo pilot stations operate through the use of voice recognition technology.

The air traffic controller stations (fig. 3) are composed of advanced computer graphics systems and host computers to provide the controller with generic, but realistic, displays. The displays can be programmed to represent present day display formats or to represent futuristic formats for research purposes. Finally, a realistic air-ground communications system is simulated to provide the real world communications environment.

TSRV SIMULATION DESCRIPTION

The ATOPS Program operates a Boeing 737-100 aircraft (fig. 4) to conduct flight research aspects of the program. The aircraft is equipped with a special research flight deck, located approximately 20 feet aft of the standard flight deck. An extensive array of electronic equipment and data recording systems is installed throughout the former passenger cabin (fig. 5). The aircraft can be flown from the aft flight deck research cockpit using advanced flight control and electronic display systems that can be programmed for research purposes. Two safety pilots located in the standard flight deck are responsible for all phases of flight safety and for most traffic clearances. Two research pilots usually fly the aircraft from the research cockpit during test periods, which can last from takeoff through landing.

Figure 6 presents a picture of the interior of the TSRV Simulator, which is a near replicate of the research cockpit located onboard the TSRV research aircraft. The simulation includes a nonlinear mathematical model of the aircraft with the addition of landing gear dynamics, gust and wind models, nonlinear actuator models, and instrument and microwave landing system (ILS and MLS) sensor models. In addition, automatic flight control and navigation control functions have also been simulated. The simulator cockpit is outfitted with advanced flight control and electronic display systems. These include an advanced guidance and control system (AGCS), an electronic attitude director indicator (EADI), an electronic horizontal situation indicator (EHSI), and a navigation control and display unit (NCDU).

The various AGCS modes are engaged using the control panel pictured in figure 7. These control modes provide the pilot with desired levels of automation and are designed to relieve the pilot's workload. The AGCS modes

include two levels of control wheel steering (attitude and velocity vector), four levels of outer loop guidance and control (track angle and flight path angle select, horizontal path guidance, vertical path guidance, and time path guidance), an autoland system, an altitude hold system, and an autothrottle system.

The EADI, pictured in figure 8 and described in reference 6, is the pilot's primary display of pitch and roll attitude for instrument flight. Optional symbology for display of the aircraft velocity vector, flight path acceleration, vertical and horizontal guidance errors, speed error, perspective runway and centerline, and radar altitude are integrated into the EADI display format.

The EHSI, pictured in figure 9 and described in reference 7, is the pilot's primary navigation display for instrument flight. It is configured to represent a map and provides the pilot with an accurate display of aircraft position relative to the horizontal guidance path, flight plan waypoints, and geographic points of interest. The desired horizontal flight plan is displayed by a solid line connecting the waypoints. The operating modes of the pilot's and copilot's EHSIs are independent and may be operated in either track-up (normal) or north-up modes and with different scales and different information options.

The primary input device to the navigation and guidance system is the NCDU pictured in figure 10. The unit consists of a keyboard and a small cathode ray tube (CRT) display on which pages of navigation and guidance information may be displayed. Guidance paths may be built using the NCDU as an input/output device. During the flight, variables of interest, such as path guidance errors, may be displayed on the CRT.

ANALYSIS

Modeling Human Performance of the Tracking Task

The experimental data has been analyzed from the standpoint of a one-dimensional tracking problem. The state variables can be regarded to be the distance traveled along a prescribed trajectory in space and its time derivative. Alternatively, the position error and its time rate of change can be the state variables, since their knowledge used with certain known information allows the distance traveled of the pilot's aircraft and its derivative to be calculated. It is assumed that other control "systems" (including pilot control actions that are not being modeled) keep the aircraft on the desired trajectory in space. The tracking task is to maintain a nominal spacing of 3 n. mi. between the pilot's aircraft and the lead aircraft by the use of speed control only.

In each of the forty flights, a pilot performed speed control on his aircraft in consideration of many factors, including the flight plan and his perception of the separation and its rate of change between his aircraft and the lead aircraft. Each experiment resulted in a state trajectory which was sampled and recorded in Regions 2 and 3 of the flight plan. The modeling problem considered herein for each flight was to find a mathematical model driven by the state variable feedback whose state trajectory approximated the state trajectory from human pilot performance.

The model

$$\ddot{Z}_0(t) = -2\zeta\omega\dot{X}(t-\tau) - \omega^2 X(t-\tau)$$

was selected after some experimentation to model performance of the tracking task. In this equation, ζ is the damping coefficient, ω is the undamped natural frequency, and τ is the delay in feeding back the state of the system. Since the definition

$$X = (Z_0 + H) - Z_1$$

includes the nominal separation H as a parameter, the acceleration of the pilot's aircraft given by the model depends on the parameter vector (ζ,ω,H,τ).

Identification Problem

The measure E_p of the position error between an experimental trajectory and a model trajectory was defined to be

$$E_p(\zeta,\omega,H,\tau) = \int(X_e(t) - X_m(t;\zeta,\omega,H,\tau))^2\ dt.$$

Similarly, the velocity error was defined as

$$E_v(\zeta,\omega,H,\tau) = \int(\dot{X}_e(t) - \dot{X}_m(t;\zeta,\omega,H,\tau))^2\ dt.$$

A weighted sum of the position and velocity errors was used as the overall error $E(\zeta,\omega,H,\tau;W_p,W_v)$:

$$E(\zeta,\omega,H,\tau;W_p,W_v) = W_pE_p(\zeta,\omega,H,\tau) + W_vE_v(\zeta,\omega,H,\tau).$$

With these measures of modeling errors, the identification problem becomes

$$\underset{(\zeta,\omega,H,\tau)}{\text{Min}} \quad E(\zeta,\omega,H,\tau;W_p,W_v) \text{ or equivalently}$$

$$\underset{(\zeta,\omega,H,\tau)}{\text{Min}} \quad \left\{W_pE_p(\zeta,\omega,H,\tau) + W_vE_v(\zeta,\omega,H,\tau)\right\},$$

which depends on the weights W_p and W_v that are used. The weight W_p is applied to the square of the difference between the position error X_m predicted by the model and the actual position error X_e from the experiment. Similarly, the weight W_v is applied to the square of the velocity error difference between model and experiment. Thus the weights $(W_p,W_v) = (1,0)$ give an error that does not explicitly depend on the velocity error match between the model and experimental data. Also, $(W_p,W_v) = (0,1)$ results in no explicit dependency of the measure of goodness of fit of the position error match between the model and the experimental data, while $(W_p,W_v) = (0.5,0.5)$ gives some weight to matching both position error and velocity error. There may be room for argument regarding the "best" weights to use in the integral square error measurement. The analysis described herein was done using the

weights $W_p = W_v = 0.5$. The resulting family of model trajectories approximate their experimental counterparts with errors that are acceptably small for many areas of model application. Of course, the judgement as to whether or not the accuracy is acceptable can be made only in consideration of the context of application of the model. If smaller modeling errors are needed for a specific application, the weights W_p and W_v can be changed to obtain new families of model trajectories.

When the weights W_p and W_v are fixed (the values $W_p = W_v = 0.5$ were used), an identification problem involving the four parameters ζ, ω, H, and τ results. If computational time were not a consideration, one could search over the four parameters to find the parameter vector which yielded the minimum value of the error $E(\zeta,\omega,H,\tau,W_p,W_v)$. Unfortunately, the system must be simulated each time the error is to be evaluated for a given parameter vector (ζ,ω,H,τ). Consequently, an approximate solution to the identification problem was sought by using the procedure:

(i) using a heuristic search in (H,τ) space to find promising values of H and τ. The equation error method was used to calculate ζ, ω and the attendant error for given values of H and τ.

(ii) searching in (ζ,ω) space for given values of H and τ to find a local minimum value of the integral squared error.

(iii) repeating steps (i) and (ii) until a reasonably good fit was obtained.

This procedure, which decomposes the search in four dimensions into two searches, each in two dimensions, was found to result in acceptable computational times. The procedure was arrived at after performing a series of numerical experiments to investigate the tradeoff between computer time and modeling error.

The equation error method was applied to the problem of selecting H and τ as follows. When H and τ are fixed, the pilot's aircraft acceleration, $\ddot{Z}_0$, predicted by the model depends only on ζ and ω. At time t_n, we have the

pilot's aircraft acceleration observed from the experiment and the pilot's aircraft acceleration predicted from the model:

$$\ddot{Z}_0(t_n) = -2\zeta\omega\dot{X}(t_n-\tau) - \omega^2 X(t_n-\tau).$$

Thus when exactly two observations (at distinct times t_m and t_n) are used, we have two equations and two unknowns, and the values of ζ and ω can be calculated provided that the resulting equations are independent. When more than two observations are used, there results an overspecified system of equations. For example, if there were exactly three distinct observations (taken at times t_1, t_2, and t_3), the system of equations is

$$\begin{bmatrix} -2\dot{X}(t_1-\tau) & -X(t_1-\tau) \\ -2\dot{X}(t_2-\tau) & -X(t_2-\tau) \\ -2\dot{X}(t_3-\tau) & -X(t_3-\tau) \end{bmatrix} \begin{bmatrix} \zeta\omega \\ \omega^2 \end{bmatrix} = \begin{bmatrix} \ddot{Z}_0\ (t_1) \\ \ddot{Z}_0\ (t_2) \\ \ddot{Z}_0\ (t_3) \end{bmatrix}$$

Assuming the observations are independent, an overspecified system of equations of the form $Au = b$ results, where

$$A = \begin{bmatrix} -2\dot{X}(t_1-\tau) & -X(t_1-\tau) \\ -2\dot{X}(t_2-\tau) & -X(t_2-\tau) \\ -2\dot{X}(t_3-\tau) & -X(t_3-\tau) \end{bmatrix}, \quad u = \begin{bmatrix} \zeta\omega \\ \omega^2 \end{bmatrix}, \text{ and } \quad b = \begin{bmatrix} \ddot{Z}_0\ (t_1) \\ \ddot{Z}_0\ (t_2) \\ \ddot{Z}_0\ (t_3) \end{bmatrix}$$

The overspecified system of linear equations represented by $Au = b$ can be "solved" in the least squared error sense by $u = (A^TA)^{-1}A^Tb$. The resulting solution u minimizes the sum of the squared errors associated with each equation. The squared error is $b^Tb-(A^Tb)^T(A^TA)^{-1}(A^Tb)$.

In summary, the equation error method enables ζ and ω to be calculated analytically when W, H and τ are fixed, as opposed to having a search over (ζ,ω) space done with the evaluation of each point in (ζ,ω) space requiring a time integral to be done to calculate its attendant error. Consequently, a two-dimensional search over H and τ can be done to find starting values for H, τ, ζ, and ω.

When W, H, and τ are fixed, the identification problem simplifies to

$$\min_{\zeta,\omega} \left\{ W_p E_p(\zeta,\omega;H,\tau) + W_v E_v(\zeta,\omega;H,\tau) \right\}$$

where $E_p(\zeta,\omega;H,\tau)$ is the time integral of the square of the difference in the position errors between the experimental and model results, and $E_v(\zeta,\omega;H,\tau)$ is defined similarly for the velocity difference.

The values of ζ and ω that result in a minimum value of the integral squared error $E(\zeta,\omega,H,\tau,W_p, W_v)$ for H and τ given were sought as follows. First of all, the equation error method was used to give initial values for ζ and ω. Then the value of the integral squared error $E(\zeta,\omega,H,\tau,W_p,W_v)$ for H and τ given was calculated by simulating the performance of the model represented by the parameters $(\zeta,\omega;H,\tau)$ in Regions 2 and 3. This simulation required the use of numerical integration. The triangular rule with a time increment of four seconds was found to yield satisfactory results. The point (ζ,ω) was accepted as a local minimum when the following conditions were met

$$E(\zeta+\Delta\zeta,\omega;H,\tau,W_p,W_v) > E(\zeta,\omega;H,\tau,W_p,W_v) - DE$$

$$E(\zeta-\Delta\zeta,\omega;H,\tau,W_p,W_v) > E(\zeta,\omega;H,\tau,W_p,W_v) - DE$$

$$E(\zeta,\omega+\Delta\omega;H,\tau,W_p,W_v) > E(\zeta,\omega;H,\tau,W_p,W_v) - DE$$

$$E(\zeta,\omega-\Delta\omega;H,\tau,W_p,W_v) > E(\zeta,\omega;H,\tau,W_p,W_v) - DE$$

that is, the new point must be better than the old point by more than DE (a fixed number) to be regarded as yielding a significantly better fit. When a new best point is found, it becomes the starting point for another similar search in the four directions. The process is continued until a local minimum is found. The parameter DE was determined experimentally by trying different values and observing their impact on the attendant modeling errors. For the triangular method of numerical integration with a time increment of four seconds, the value DE = 0.20 was found to yield satisfactory results.

DESCRIPTION OF EXPERIMENTS

A factorial design of experiments was used with four pilots, two control systems, and five replications for a total of forty experiments. Four separate pilots were used in anticipation of task performance dependency on the person performing the task. The two control systems - velocity vector control wheel steering (VCWS) and 3D automatic flight path guidance and control both coupled with manual throttles - result in different work loads. The VCWS requires the pilot to perform certain control tasks related to maintaining his aircraft on the desired trajectory in space which are done automatically in the 3D control mode. The workload under VCWS could conceivably be detrimental if it prohibits the pilot from giving enough attention to the tracking task. On the other hand the light workload under 3D could be detrimental if it is insufficiently demanding to hold the pilot's concentration. Five replications were used for each combination of pilot and control system to allow measurement of variation within each cell.

For a given test run, the pilot was instructed to try to maintain a separation of 3 n. mi. between his aircraft and the lead aircraft. This was to be accomplished primarily through speed variation by use of the throttles, speed brakes, and flaps. Both aircraft used the same flight plan, and it was displayed to the pilot on the EHSI. Since the flight plan (fig. 11) involved a constant speed and altitude segment followed by a deceleration segment, a descent segment and, finally, a turn, the pilot knew in advance that it would be impossible for him to maintain the 3 n. mi. spacing. The pilot was told that his aircraft would start out "in trim" with no position or velocity errors. That is, the controls would initially be set for maintaining the conditions of airspeed and altitude required by the flight plan in the first region. A CDTI display, presented on the EHSI, supplied the pilot with

information regarding the separation between his aircraft and the lead aircraft. The display was updated at four second intervals and contained range circles at 2 and 4 n. mi. to help the pilot maintain his 3 n. mi. separation. Each pilot was offered a trial run before his first replication; the only pilot to refuse was the one who had originally made the run which generated the data for the target aircraft which was used in these experiments. A copilot was available to handle flap configuration changes when called for by the pilot.

The flight plan, shown in figure 11, can be described in terms of regions. The aircraft was to cruise at 250 kts and 14,000 feet altitude at a track angle of 135^{o} in Region 1. In Region 2, the altitude and track angle were to be maintained while decelerating from 250 to 200 kts airspeed. Then the airspeed and track angle were to be maintained while descending to 11,000 feet in Region 3. This was followed by a period of flying at 200 kts and 11,000 feet in Region 4, again with the same track angle. Region 5 required a left turn to a new track angle of 0^{o}, and Region 6 was a straight run at a constant airspeed of 200 kts and a constant altitude of 11,000 feet to the threshold of the runway.

The data logged for each experiment include the average and RMS values of the separation and its rate of change between the two aircraft in each of the six regions. Detailed data were recorded each half second in Regions 2 and 3 on the pilot's aircraft and the lead aircraft for position and groundspeed. This detailed data can be used to describe the state trajectory in the regions of deceleration and descent of the flight plan. Regions 2 and 3 were selected for the collection of detailed data to allow for modeling to be done of the tracking task during deceleration and descent. Regions 1 and 4, both of which involve cruising at constant speed and altitude, surround the regions of

detailed data collection and thus allow time for the damping out of any transient effects associated with simulation startup or the completion of the simulation. Thus the state trajectory data were available for parameter identification, while average and RMS data were available to allow a comparison between model-generated and experimental state trajectories in Regions 2 and 3.

RESULTS AND DISCUSSION

The first section summarizes the results of a data analysis performed prior to modeling the human pilot performance of the tracking task. This preliminary analysis concentrates on eight response variables which are aggregate statistics on the task performance in Regions 2 and 3 of the flight plan. The response variables are the average and RMS deviations of the separation between the two aircraft and of the groundspeed for the pilot's aircraft in the two regions. The second section discusses the sensitivity of fit to the model parameters. The third section assesses the validity of the models obtained by solving the forty modeling problems. The final section presents a summary of the model parameter values and describes a structure that can be used for the general problem of modeling human pilot performance of the tracking task.

Preliminary Analysis of Data

This part of the overall data analysis problem investigates the importance of the three factors (pilot, control system, and replication number) on the response variables (average and RMS of aircraft separation distance and of the groundspeed for the pilot's aircraft for Regions 2 and 3). The second and third parts of the overall data analysis problem, which are concerned with model verification and the analysis of model parameter distributions, are described in later sections of this report.

Let A_{edj} denote the experimental average separation between the target and the pilot's aircraft in Region j (j=2,3) for the experiments (e for experiments, d for separation distance), and let R_{edj} denote the experimental RMS deviation for the separation in Region j. Define A_{evj} and R_{evj} similarly for the experimental average and RMS deviation for the groundspeed of the pilot's aircraft in Region j. These eight response variables may in general depend on the three independent variables specifying the pilot, control system, and replication number.

An analysis of variance (ANOVA, ref. 8) was performed to investigate the significance of the three factors upon the eight response variables. Table 1 indicates that the type of control system is not a statistically significant factor for any of the eight response variables when the level of significance is 1 percent. Consequently, the sum of squares from the type of control system is pooled with the residual sum of squares in the ANOVA that follows.

Table 2 summarizes the results for a two-way ANOVA on the eight response variables for Regions 2 and 3. Sums of squares from two-way interactions, which were not statistically significant, are pooled into the residual sum of squares to obtain Table 2. Table 2 shows that the pilot effect is statistically significant ($\alpha<.05$) for six of the eight response variables. In

addition, four of the variables are also statistically significant at the $\alpha = .01$ level. The table also shows that the replication number is statistically significant for three of the eight response variables at the 5 percent level of significance and for one variable at the 1 percent level. This evidence indicates that the replication number is less important than the pilot in its effect on the response variables. A breakdown by replication number of the sample means and standard deviations is given in Table 3, and a breakdown by pilot is given in Table 4. Thus the preliminary analysis of the data indicates that any model of pilot performance must have a structure which can accommodate the variability of task performance with the pilot and his experience at performing the tracking task.

Sensitivity of Fit to Model Parameters

The mathematical model has four parameters - H, τ, ζ, and ω - which can be selected to cause a model state trajectory to approximate an experimental state trajectory. It was found from experience that the errors in the approximation depend strongly on the nominal spacing H. Indeed, large errors resulted for most of the forty experiments when H = 3.0 was fixed a priori, rather than having H selected to match trajectories.

By contrast, the goodness of fit was relatively insensitive to the delay τ in feeding back the position and velocity differences. The delay could in many cases be increased by four or even eight seconds without markedly increasing the error in the fit of the model output to the experimental data. The sensitivity of the fit to the parameters ζ and ω tended to lie between the high sensitivity to H and the low sensitivity to τ.

Model Validation

Each of the forty flights resulted in a trajectory which was modeled by selecting the parameters ζ, ω, H, and τ in the model structure

$$\ddot{Z}_0(t) = -2\zeta\omega\dot{X}(t-\tau) - \omega^2 X(t-\tau),$$

where X(t) depends implicitly on H. Thus there were forty different models of task performance, all having the same structure but each having its unique parameter vector (ζ, ω, H, τ).

Table 5 summarizes the results that were obtained. The preliminary analysis of data indicates that performance depends upon the pilot involved and his experience at performing the tracking task. This dependency can be modeled by regarding the parameter vector (ζ, ω, H, τ) to be a random selection from an event space consisting of all parameter vectors which may possibly result. Thus the fact that no two state trajectories will be identical, even for a pilot with extensive experience at performing the tracking task, is reflected in the model by the fact that no two parameter vectors selected at random are likely to be identical.

Two major questions appear to dominate concerns regarding model validity. One question addresses the match of the state trajectory from a model to the state trajectory used to identify the parameters in that model. The question may be phrased as "Does the model $\ddot{Z}_0(t) = -2\zeta\omega\dot{X}(t-\tau) - \omega^2 X(t-\tau)$, where ζ, ω, H, and τ are chosen in consideration of the experimental data for a specific simulation run, yield a satisfactory fit to the experimental data?" This section of this report presents evidence that the model is valid in this sense. A second question addresses the match of the family of state trajectories, which result from the use of values of ζ, ω, H, and τ selected as random samples from distributions estimated from the data in Table 5, to

the family of state trajectories that will be obtained from pilots selected at random to perform the tracking task. This question may be phrased as "Does the model $\ddot{Z}_0(t) = -2\zeta\omega\dot{X}(t-\tau) - \omega^2 X(t-\tau)$, where ζ, ω, H, and τ are selected at random from distributions based on the data in Table 5, yield trajectories which are representative of those which will be obtained by having human pilots perform the tracking task?" This question appears to require further research.

The following material is concerned with the validity of the use of the model $\ddot{Z}_0(t)=-2\zeta\omega\dot{X}(t-\tau) - \omega^2 X(t-\tau)$, where ζ, ω, H, and τ are chosen in consideration of experimental data from a specific simulation run, to fit the experimental data for that run.

Graphical Comparison.- The plots in figures 12 through 15 illustrate graphically the errors that result. Experimental and model values are plotted as a function of time for both the separation and the velocity difference between the lead aircraft and the pilot's aircraft. Remarkably good fits were obtained for many of the forty experiments that were performed. For example, a visual inspection of figures 12 and 13 leaves little doubt that the model results in an excellent approximation to the separations and velocities from those experiments. The poorest fits include those presented in figures 14 and 15. However, the following statistical analysis of model validity includes these relatively poor fits. Fortunately, the pilot and experience effects dominate the modeling errors even when these data are included in the statistical analysis.

Statistical Analysis for Model Verification.- A statistical assessment of model validity is next made by comparing the response variables from the experimental data to their values from the models. Additional notation must be introduced to explain these results on model verification. As before, the

eight experimental response variables are A_{eij} and R_{eij}, where i=d,v (distance or velocity), and j=2,3 (Region 2 or 3). The modeling results in a corresponding set of response variables A_{mij} and R_{mij}. Each of the forty experiments yielded experimental values for the eight response variables A_{eij} and R_{eij}, while each of the forty modeling problems yielded model output values for the variables A_{mij} and R_{mij}.

ANOVA Comparing Pilot, Experience and Modeling Effects.- The preliminary analysis in the first section of the Results and Discussion indicates that the model of pilot performance must have a structure which can accommodate variability of task performance with the pilot and his experience at performing the task. A comparison of the modeling errors with the pilot and experience effects can be made by performing the calculations for a three-way analysis of variance (pilot effect, experience effect, model data versus experimental data effect) for each response variable. Table 6 summarizes the results with two-way and higher order interactions, which were found to not be significant, pooled into the residual sum of squares. In Table 6, the first response variable refers to the average separation in Region 2 as determined by either the test runs or the models. For example, each of the five replications for the four pilots resulted in an experimentally determined average separation A_{ed2} in Region 2; each also resulted in an average separation A_{md2} determined by its model. Thus there are five replications, four levels for the pilots, and two levels for the source of the data (model versus experimental).

The data in Table 6 shows that the modeling effect is small compared to the effects due to the pilot and his experience at performing the tracking task. Indeed, the null hypothesis that there is no modeling effect is

rejected for two of eight response variables when the level of significance is .05 and is also rejected for three of eight response variables when the level of significance is as high as .15.

Student's t Test by Pairs on Modeling Errors.- Table 7 summarizes the results for model verification via a statistical comparison of the response variables. The leftmost column gives the algebraic difference in the sample means of the response variables. For example, this difference is $M(A_{md2})$-$M(A_{ed2})$ = 3.218-3.228 = -0.010 n. mi. for the difference between the model output and the experimental results for the average separation in Region 2. The percentage difference, given in the middle column, is the ratio (expressed in percent) of the algebraic difference in the means to the mean value for the experiments, $\left\{\frac{M(A_{md2}) - M(A_{ed2})}{M(A_{ed2})}\right\} \times 100\%$. For the average separation in Region 2, this is -0.3%. The level of significance in Table 7 corresponds to a paired two-sample t test.

The null hypothesis that the population mean for the model output equals the population mean for the experimental data is accepted at the .05 level of significance for the differences A_{md2}-A_{ed2}, A_{mv2}-A_{ev2}, R_{mv2}-R_{ev2}, A_{md3}-A_{ed3}, R_{md3}-R_{ed3} and R_{mv3}-R_{ev3}. However, the null hypothesis is rejected for the average velocity difference A_{mv3}-A_{ev3} in Region 3 and the RMS deviation for separation R_{md2}-R_{ed2} in Region 2. The difference between the model outputs and experimental data for the average velocity in Region 3 has a strong statistical significance. Fortunately, this statistically significant difference may not be practically significant. The error is only two knots, which is an error of less than 1 percent in the mean groundspeed. Similarly, the statistically significant difference between the model and experimental data for the RMS deviation of the separation in Region 2 may also result in acceptably accurate approximations for many applications of the model. The

difference in RMS deviation for the separation is only 0.021 n. mi., or roughly 39 meters. This is less than a sixteen percent error of the experimental RMS deviation of 0.136 n. mi.

In summary, the parameters in the model $\ddot{Z}_0(t) = -2\zeta\omega\dot{X}(t-\tau) - \omega^2 X(t-\tau)$ can be selected to cause the state trajectory from the model to approximate the state trajectory from human pilot performance. Consequently, human performance of this tracking task in a MOTAS environment can be modeled by using a model with this structure. The problem is addressed next of selecting the model parameters ζ, ω, H, and τ to result in a representation of the variety of human responses that can reasonably be expected to occur.

Using the Model in a MOTAS Simulation

These results can be applied as follows to model human performance of this tracking task. There was no strong evidence that the four parameters were statistically dependent. Consequently, the modeling information from the forty experiments is summarized in terms of separate distributions for H, τ, ζ, and ω which are given in figures 16 through 19. Human performance of this tracking task can be simulated by obtaining a random parameter vector from the distributions of H, τ, ζ, and ω and using it to define a model which is integrated to obtain its state trajectory. To illustrate a method which can be used, assume that a CDTI-equipped aircraft with the tracking task has entered a MOTAS-type simulation. A model of the aircraft's performance of its tracking task is

$$\ddot{Z}_0(t) = -2\zeta\omega\dot{X}(t-\tau) - \omega^2 X(t-\tau)$$

where H, τ, ζ, and ω are from the distributions in figures 16 through 19. Assuming that R is a random sample from a uniform distribution over (0,1), a value of ζ (for example) is determined as the value for which the cumulative distribution function in figure 18 equals R. In equation form, the value of ζ is chosen so that CDF(ζ) = R. Random values for H, τ, and ω can be determined similarly by using the data in figures 16, 17, and 19 respectively to transform an independent sample R from a uniform distribution over (0,1) into a random variable (H, τ, or ω) from a distribution having the appropriate shape. Thus the results can be incorporated into a model of air traffic in the terminal area to simulate human performance of CDTI-equipped aircraft performing the tracking task.

CONCLUDING REMARKS

The data from forty tracking experiments have been used to model human performance of the tracking task. The experimental results were found to depend on the pilot and his experience at performing the task. The performance for each experiment was modeled by using a second-order differential equation with parameters (ζ, ω, H, and τ). A heuristic search was used to identify H and τ, while a systematic search in (ζ, ω) space was used for H and τ given to find a local solution to the simplified identification problem. A family of forty parameter vectors (ζ, ω, H, τ) results from solving the identification problem for the forty experiments. The errors resulting from the use of these parameters in modeling human pilot performance are acceptably small for many areas of application. Of course, final judgement as to model validity must be made in consideration of the context in which the model is to be used. If the accuracy reported herein appears to be unsatisfactory for a particular application, greater accuracy may be obtained by using different weights on the position and velocity errors (the weights W=(0.5,0.5) were used), and by using different starting points with a smaller step size in searching over the parameter space.

The problem of modeling human performance of this tracking task in a MOTAS environment goes beyond the above-mentioned problem of identifying model parameters to approximate a given state trajectory. Rather, one must determine the model parameters in a way that results in a family of state trajectories from the model that are representative of the family of state trajectories which would result from human performance. The research reported herein has established the validity of the model structure; in addition, a method has been described for translating information on the probability

distributions of the model parameters ζ, ω, H, and τ into specific models of human performance. However, additional experimentation involving other pilots may be required to obtain more confidence in these probability distributions than is allowed by basing them on only forty experiments.

REFERENCES

1. Staff of NASA Langley Research Center and Boeing Commerical Airplane Company: Terminal Configured Vehicle Program - Test Facilities Guide. NASA SP-435, 1980.

2. Kaylor, Jack T.; Simmons, Harold I.; Naftel, Patricia B.; Houck, Jacob A.; and Grove, Randall D.: The Mission Oriented Terminal Area Simulation Facility. NASA TM-87621, 1985.

3. Credeur, Leonard; Davis, Christina M.; and Capron, William R.: Evaluation of Microwave Landing System (MLS) Effect on the Delivery Performance of a Fixed-Path Metering and Spacing System. NASA TP-1844, 1981.

4. Houck, Jacob A.: A Simulation Study of Crew Performance in Operating an Advanced Transport Aircraft in an Automated Terminal Area Enviornment. NASA TM-84610, 1983.

5. Naftel, Patricia B.: The Mission Oriented Terminal Area Model. NASA CR-172220, 1984.

6. Gandelman, Jules; and Holden, Robert: A Pilot Training Manual for the Terminal Configured Vehicle Electronic Attitude Director Indicator. NASA CR-159195, 1980.

7. Houck, Jacob A.: A Pilot Training Manual for the Terminal Configured Vehicle Electronic Horizontal Situation Indicator. NASA TM-81959, 1981.

8. Hicks, Charles R.: Fundamental Concepts in the Design of Experiments. Holt, Rinehart and Winston, Inc., c. 1964.

TABLE 1. - LEVELS OF SIGNIFICANCE FOR TYPE OF CONTROL SYSTEM

Region 2		Region 3	
Variable	α	Variable	α
A_{ed2}	.12	A_{ed3}	.49
R_{ed2}	.38	R_{ed3}	.27
A_{ev2}	.41	A_{ev3}	.28
R_{ev2}	.49	R_{ev3}	.05

TABLE 2. - LEVELS OF SIGNIFICANCE FOR PILOT AND REPLICATION NUMBER

Region 2			Region 3		
Response Variable	Pilot α	Replicates α	Response Variable	Pilot α	Replicates α
A_{ed2}	.000	.002	A_{ed3}	.000	.089
R_{ed2}	.043	.371	R_{ed3}	.017	.015
A_{ev2}	.002	.815	A_{ev3}	.096	.727
R_{ev2}	.078	.038	R_{ev3}	.000	.129

TABLE 3. - STATISTICS ON EIGHT RESPONSE VARIABLES BROKEN DOWN BY REPLICATION NUMBER

	A_{ed2}	R_{ed2}	A_{ev2}	R_{ev2}	A_{ed3}	R_{ed3}	A_{ev3}	R_{ev3}
Replicate 1								
Mean	3.46	.176	289.	8.8	3.39	.232	229.	14.7
Standard Deviation	.17	.077	7.	5.7	.15	.088	4.	6.7
Replicate 2								
Mean	3.26	.134	280.	18.3	3.36	.147	240.	17.3
Standard Deviation	.09	.015	8.	9.0	.26	.135	6.	21.1
Replicate 3								
Mean	3.33	.143	277.	20.2	3.25	.162	243.	14.1
Standard Deviation	.26	.037	10.	14.8	.21	.020	11.	9.5
Replicate 4								
Mean	3.22	.133	282.	20.3	3.17	.108	241.	8.2
Standard Deviation	.15	.062	9.	8.5	.28	.034	7.	2.3
Replicate 5								
Mean	3.19	.145	286.	18.4	3.17	.133	237.	12.2
Standard Deviation	.19	.075	8.	7.8	.23	.077	5.	10.1
Replicate 6								
Mean	3.21	.145	281.	23.2	3.81	.105	242.	7.9
Standard Deviation	.21	.070	12.	3.8	.25	.026	8.	5.0
Replicate 7								
Mean	3.16	.139	283.	23.4	3.24	.153	238.	13.2
Standard Deviation	.24	.067	10.	10.4	.20	.104	8.	8.2
Replicate 8								
Mean	3.14	.163	286.	23.1	3.15	.104	238.	7.2
Standard Deviation	.16	.090	10.	5.7	.14	.040	7.	2.8
Replicate 9								
Mean	3.17	.085	277.	23.5	3.22	.079	244.	5.3
Standard Deviation	.20	.018	5.	2.1	.20	.055	6.	2.3
Replicate 10								
Mean	3.15	.101	279.	24.2	3.25	.060	241.	6.1
Standard Deviation	.10	.025	6.	2.4	.18	.015	4.	5.5
All Replications								
Mean	3.23	.136	282.	20.3	3.24	.128	239.	10.6
Standard Deviation	.19	.058	9.	8.3	.20	.078	7.	8.9

TABLE 4. - STATISTICS ON EIGHT RESPONSE VARIABLES BROKEN DOWN BY PILOT

	A_{ed2}	R_{ed2}	A_{ev2}	R_{ev2}	A_{ed3}	R_{ed3}	A_{ev3}	R_{ev3}
Pilot 1								
Mean	3.05	.103	273.	21.4	3.04	.120	244.	12.6
Standard Deviation	.18	.032	5.	7.7	.19	.090	7.	5.6
Pilot 2								
Mean	3.30	.175	286.	22.9	3.40	.186	237.	18.5
Standard Deviation	.11	.072	9.	9.7	.15	.080	7.	12.8
Pilot 3								
Mean	3.25	.136	284.	15.0	3.19	.111	238.	6.7
Standard Deviation	.18	.053	7.	8.2	.13	.068	8.	3.4
Pilot 4								
Mean	3.32	.132	283.	22.0	3.33	.095	238.	4.6
Standard Deviation	.15	.051	7.	5.7	.12	.043	6.	2.4
All Pilots								
Mean	3.23	.136	282.	20.3	3.24	.128	239.	10.6
Standard Deviation	.19	.058	9.	8.3	.20	.078	7.	8.9

TABLE 5. - MODEL PARAMETER VALUES FOR THE FORTY FLIGHTS

Run No.	Pilot	Control System	Replication Number	H	τ	ζ	ω
10	1	VCWS	1	3.60	16.0	0.253	0.0264
23	1	VCWS	2	3.25	24.0	0.134	0.0261
24	1	VCWS	3	3.20	24.0	0.014	0.0300
25	1	VCWS	4	3.00	0.0	0.347	0.0384
26	1	VCWS	5	3.00	0.0	0.076	0.0374
42	1	3D	6	3.05	28.0	0.249	0.0362
43	1	3D	7	3.05	20.0	0.465	0.0322
44	1	3D	8	3.00	8.0	0.092	0.0379
45	1	3D	9	3.00	0.0	0.052	0.0387
46	1	3D	10	3.10	24.0	0.076	0.0329
Averages				3.13	14.4	0.176	0.0336
Standard Deviations				0.19	11.3	0.147	0.0049
30	2	3D	1	3.30	0.0	0.106	0.0279
32	2	3D	2	3.50	12.0	0.117	0.0341
33	2	3D	3	3.45	16.0	0.515	0.0316
34	2	3D	4	3.35	0.0	0.315	0.0270
35	2	3D	5	3.50	16.0	0.333	0.0270
36	2	VCWS	6	3.45	12.0	0.506	0.0257
38	2	VCWS	7	3.55	0.0	0.171	0.0249
39	2	VCWS	8	3.20	8.0	0.370	0.0270
40	2	VCWS	9	3.40	0.0	0.437	0.0394
41	2	VCWS	10	3.40	0.0	0.149	0.0332
Averages				3.41	6.4	0.302	0.0298
Standard Deviations				0.10	7.1	0.148	0.0046
3	3	3D	1	3.40	0.0	0.179	0.0251
4	3	3D	2	3.35	0.0	0.181	0.0276
20	3	VCWS	3	3.80	8.0	-0.019	0.0114
21	3	VCWS	4	3.20	0.0	0.566	0.0212
22	3	VCWS	5	3.30	0.0	0.308	0.0195
47	3	3D	6	3.10	0.0	0.453	0.0276
48	3	3D	7	3.20	8.0	0.438	0.0263
49	3	3D	8	3.30	8.0	0.364	0.0316
50	3	VCWS	9	3.30	12.0	0.459	0.0316
51	3	VCWS	10	3.30	0.0	0.081	0.0400
Averages				3.33	3.6	0.301	0.0262
Standard Deviations				0.19	4.8	0.189	0.0078
13	4	3D	1	3.65	0.0	0.329	0.0228
14	4	VCWS	2	3.45	0.0	0.523	0.0277
15	4	3D	3	3.30	0.0	0.292	0.0257
16	4	VCWS	4	3.50	0.0	0.007	0.0387
17	4	3D	5	3.30	0.0	0.890	0.0230
18	4	VCWS	6	3.45	0.0	-0.031	0.0400
19	4	3D	7	3.30	8.0	0.332	0.0346
27	4	3D	8	3.35	0.0	0.500	0.0230
28	4	VCWS	9	3.35	0.0	0.256	0.0293
29	4	VCWS	10	3.30	0.0	0.349	0.0286
Averages				3.40	0.8	0.345	0.0294
Standard Deviations				0.12	2.5	0.262	0.0064
Overall Averages				3.31	6.3	0.281	0.0297
Overall Standard Deviations				0.19	8.6	0.197	0.0064

TABLE 6. - COMPARISON OF PILOT EFFECT AND REPLICATION NUMBER EFFECT TO MODELING EFFECT

Response Variable	Pilot Effect α	Replication No. Effect α	Modeling Effect α
Average Separation, Region 2	.000	.000	.212
RMS Separation, Region 2	.000	.000	.000
Average Groundspeed, Region 2	.000	.000	.857
RMS Groundspeed, Region 2	.000	.000	.152
Average Separation, Region 3	.000	.000	.341
RMS Separation, Region 3	.000	.000	.087
Average Groundspeed, Region 3	.000	.000	.000
RMS Groundspeed, Region 3	.000	.000	.799

TABLE 7. - STATISTICAL COMPARISON OF RESPONSE VARIABLES FROM MODEL AND EXPERIMENTS

Response Variables	Difference in Means		Level of Significance α
	Algebraic	Percent	
$A_{md2}-A_{ed2}$	-0.01	- 0.3%	.176
$R_{md2}-R_{ed2}$	-0.02	-15.9%	.000
$A_{mv2}-A_{ev2}$	0.05	0.0%	.874
$R_{mv2}-R_{ev2}$	-1.06	- 5.1%	.138
$A_{md3}-A_{ed3}$	0.01	0.2%	.342
$R_{md3}-R_{ed3}$	-0.01	- 7.8%	.116
$A_{mv3}-A_{ev3}$	-2.00	- 0.8%	.001
$R_{mv3}-R_{ev3}$	-0.15	- 3.0%	.817

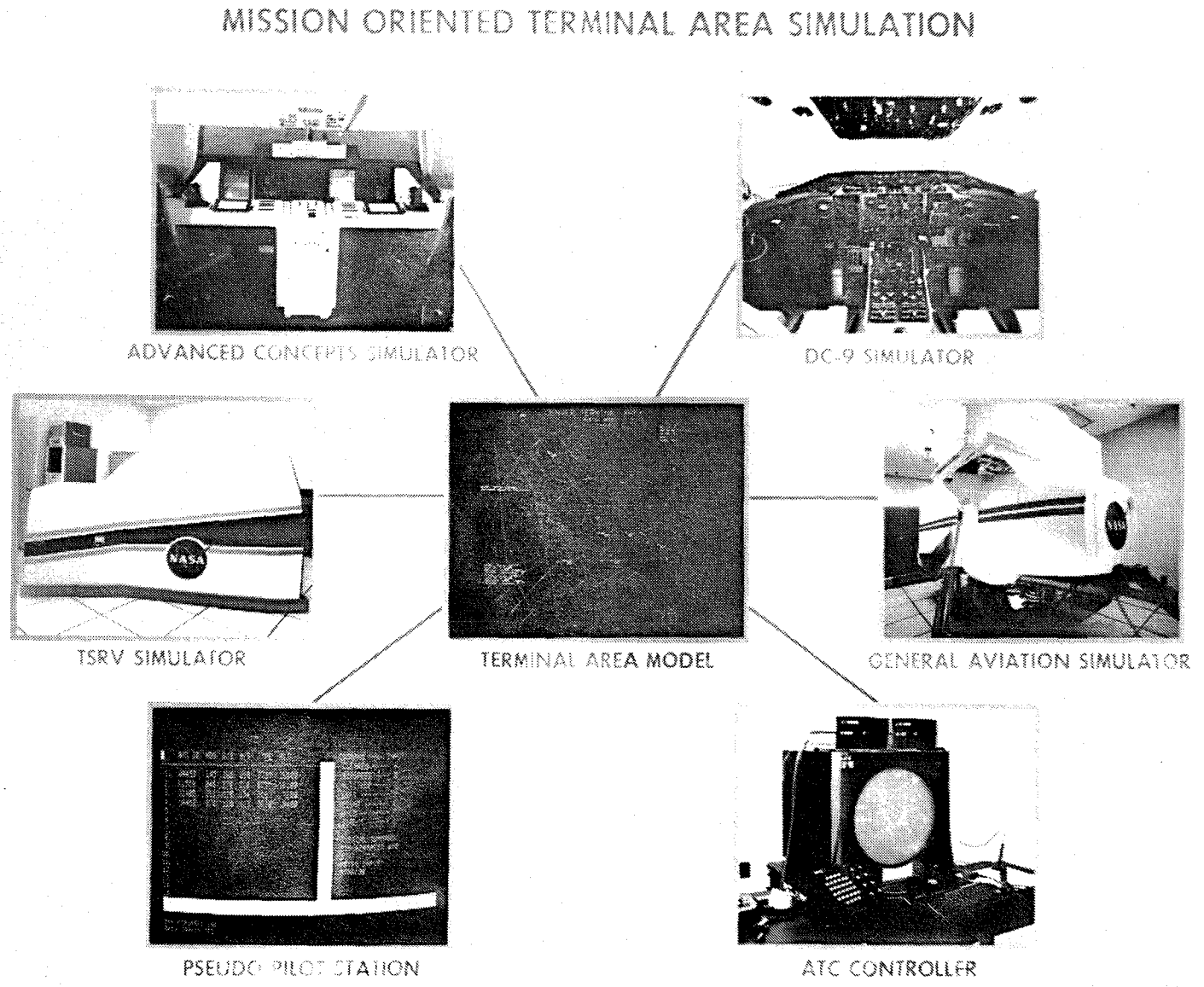

Figure 1. - Mission Oriented Terminal Area Simulation.

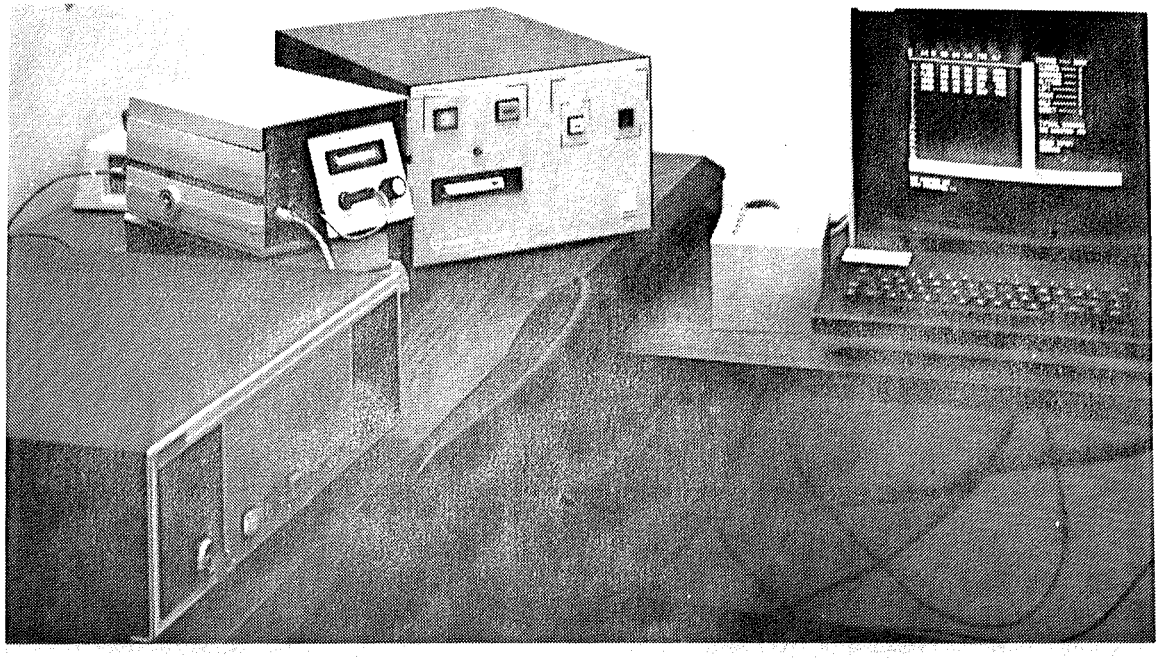

Figure 2. - Pseudo Pilot Station.

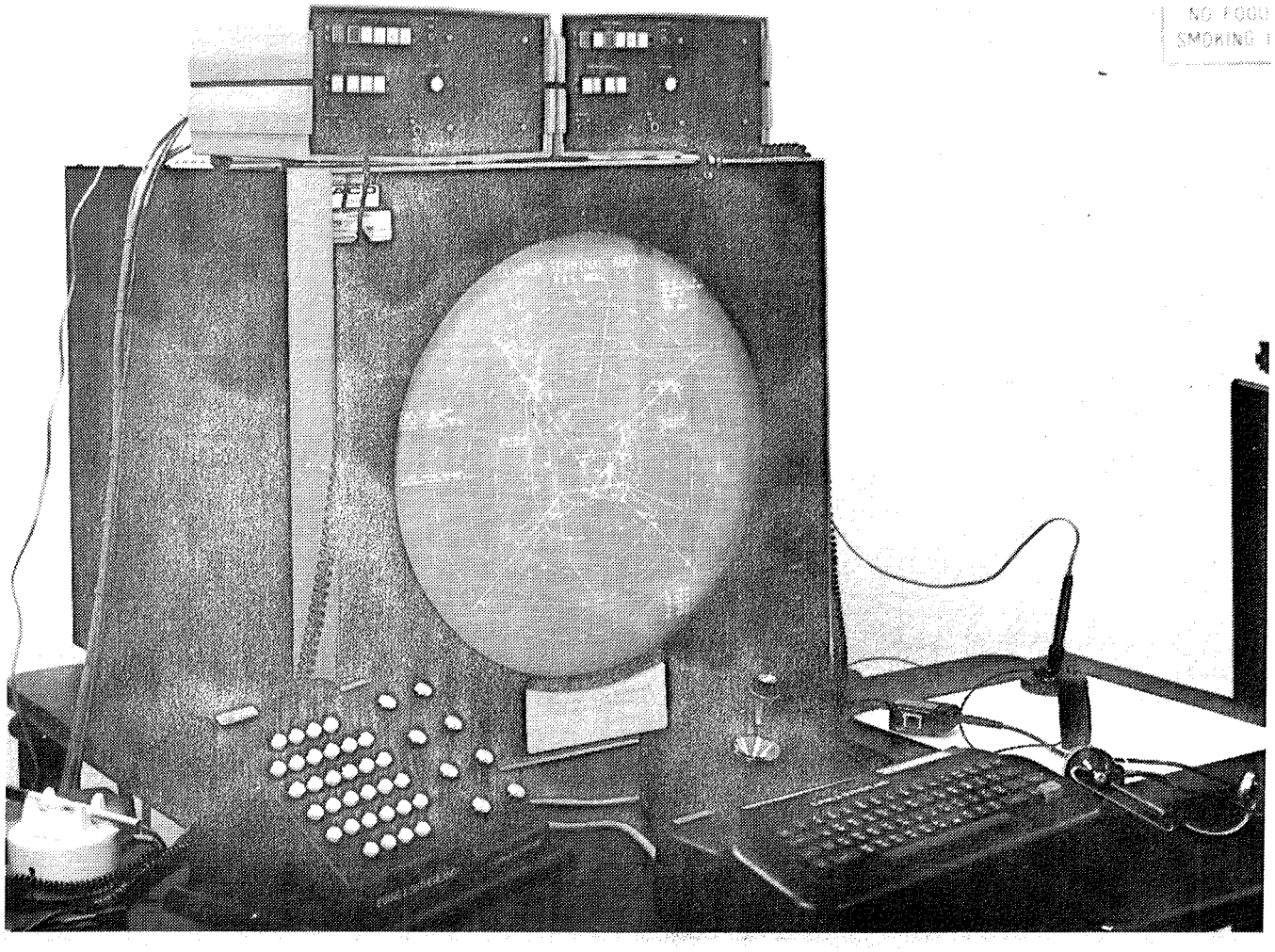

Figure 3. - Air Traffic Control Station.

Figure 4. - ATOPS B-737-100 research aircraft.

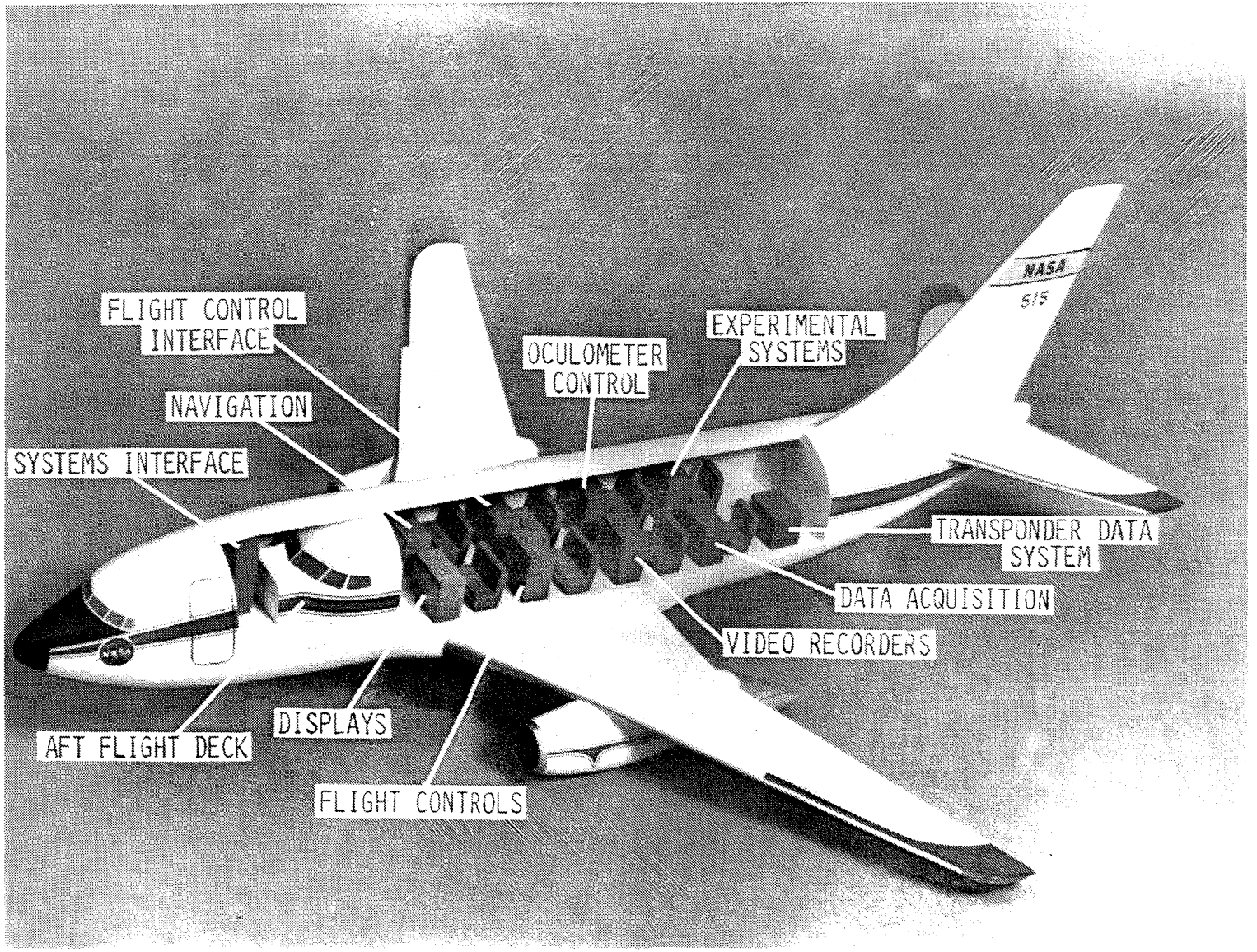

Figure 5. - Internal arrangement of ATOPS B-737-100 research aircraft.

Figure 6. - TSRV simulator cockpit.

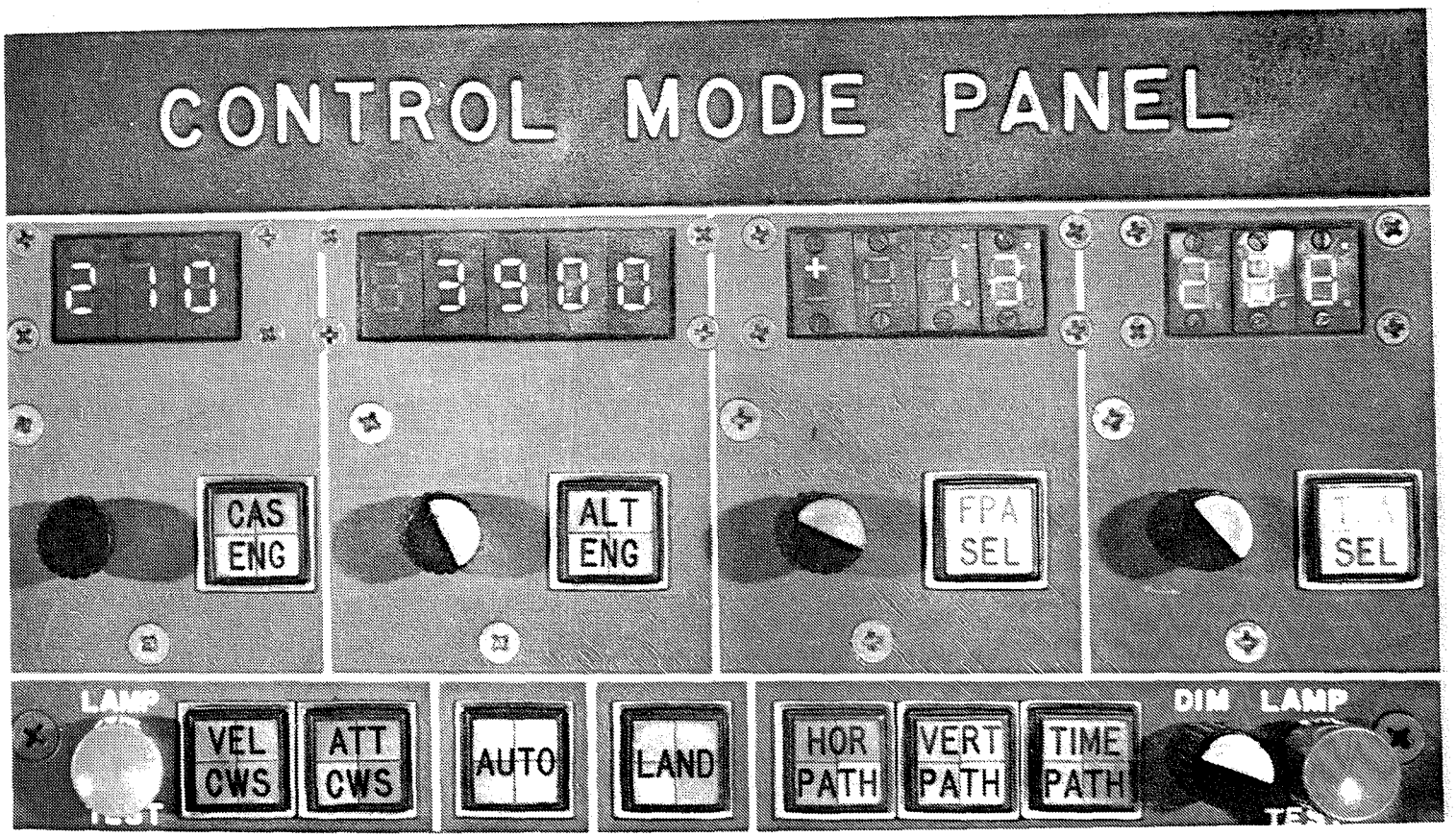

Figure 7. - Advanced guidance and control system control panel.

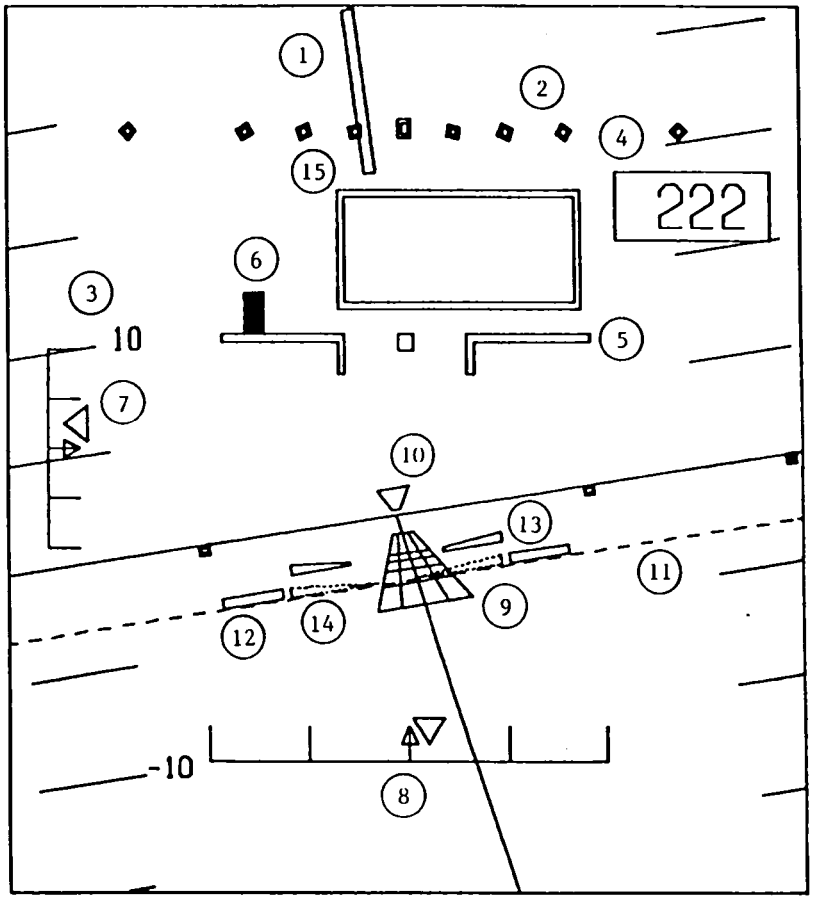

(1) Roll pointer
(2) Roll scale
(3) Pitch grid
(4) Radar altitude
(5) Aircraft reference symbol
(6) Speed error indicator
(7) Glide-slope error indicator
(8) Localizer errorindicator
(9) Runway symbol
(10) Track pointer
(11) Pitch reference line
(12) Flight-path acceleration
(13) Flight-path angle
(14) Reference flight-path angle
(15) ILS box

Figure 8. - Electronic attitude director indicator.

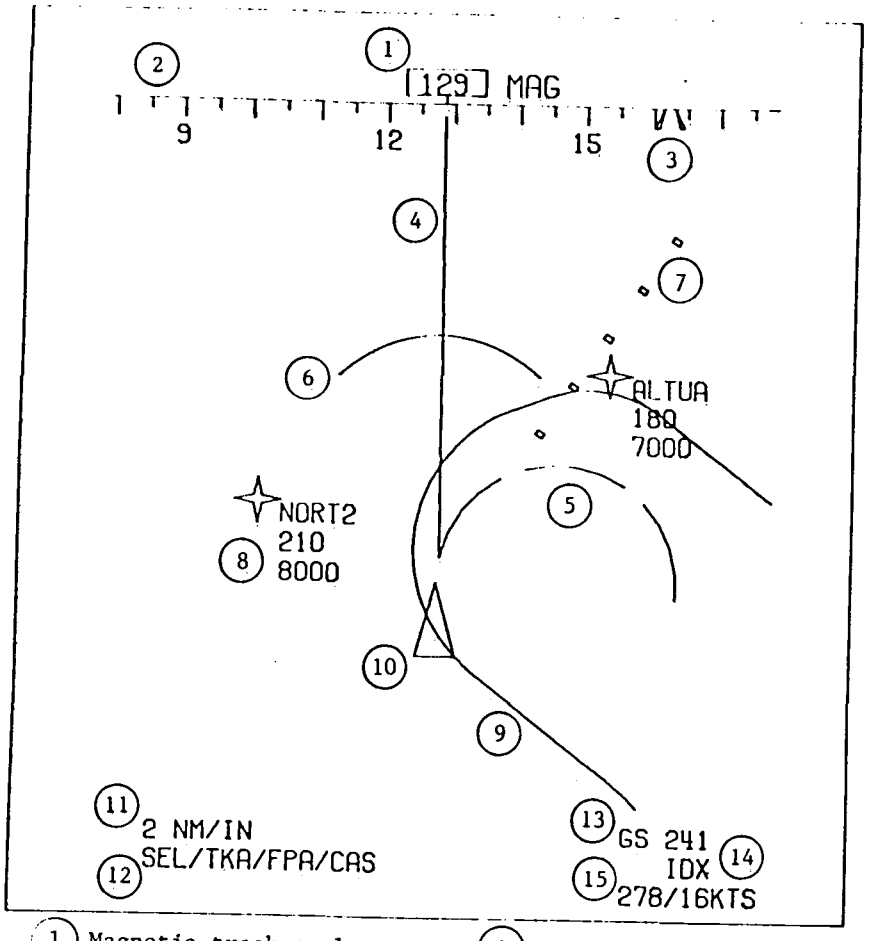

1. Magnetic track angle
2. Magnetic track angle scale
3. Track bug
4. Straight trend vector
5. Curved trend vector
6. Altitude-range arc
7. Track select dots
8. Waypoint name
   Ground speed
   Altitude
9. Flight plan
10. Aircraft symbol
11. Map scale
12. Control mode
13. Ground speed
14. Navigation mode
15. Wind direction/speed

Figure 9. - Electronic horizontal situation indicator.

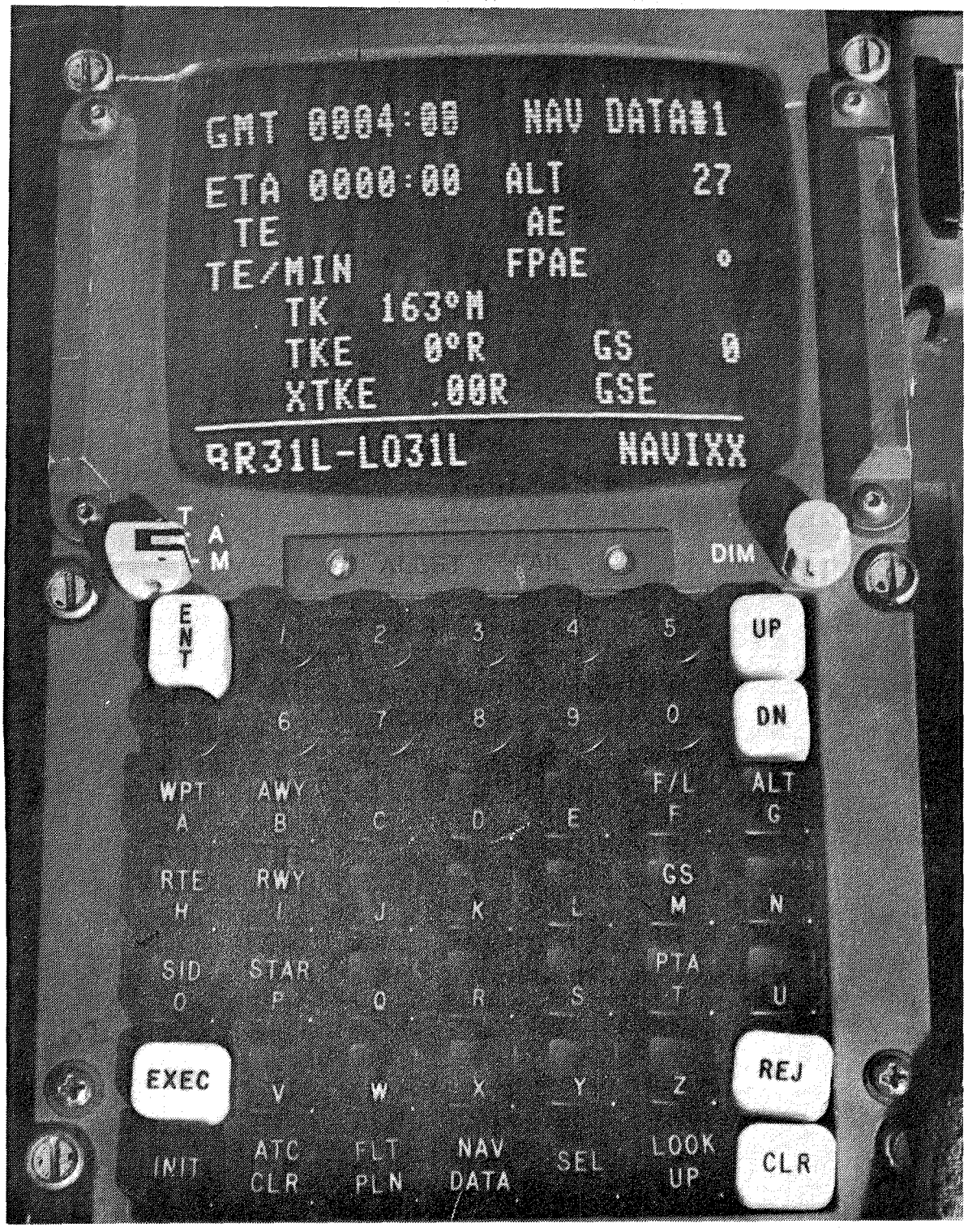

Figure 10. - Navigation control and display unit.

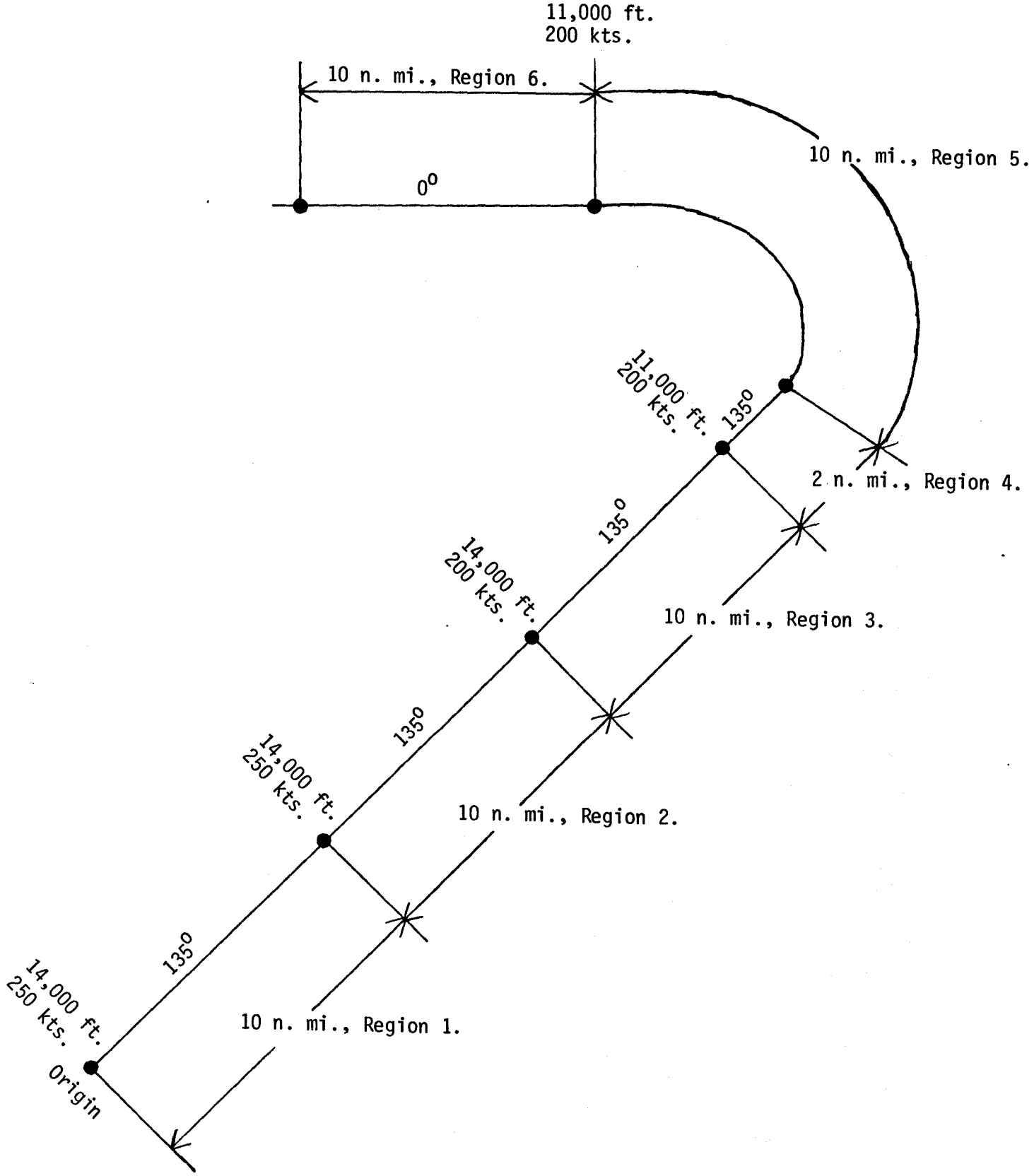

Figure 11. - Flight plan for experiments.

TIME	EX X	MO X
104.00	3.646	3.646
112.00	3.687	3.688
120.00	3.714	3.712
128.00	3.720	3.722
136.00	3.695	3.696
144.00	3.658	3.645
152.00	3.614	3.579
160.00	3.563	3.505
168.00	3.505	3.429
176.00	3.441	3.355
184.00	3.372	3.288
192.00	3.300	3.228
200.00	3.231	3.177
208.00	3.170	3.137
216.00	3.121	3.107
224.00	3.087	3.091
232.00	3.070	3.087
240.00	3.072	3.096
248.00	3.089	3.117
256.00	3.121	3.144
264.00	3.175	3.185
272.00	3.251	3.248
280.00	3.315	3.305
288.00	3.366	3.349
296.00	3.409	3.387
304.00	3.444	3.420
312.00	3.474	3.449
320.00	3.491	3.475
328.00	3.496	3.493
336.00	3.488	3.501
344.00	3.478	3.501
352.00	3.467	3.496
360.00	3.456	3.489
368.00	3.443	3.480
376.00	3.432	3.470
384.00	3.422	3.460
392.00	3.414	3.449
400.00	3.407	3.442

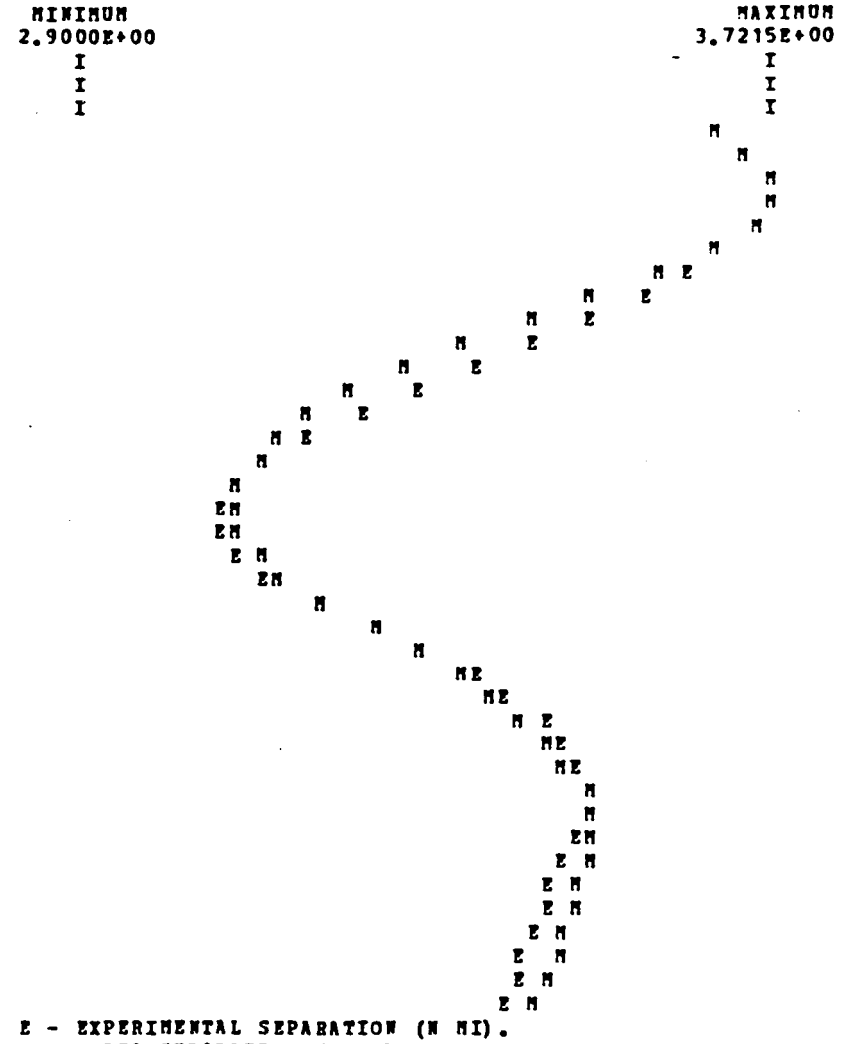

a. Separation data.

Figure 12. - Comparison of experimental and model data.

TIME	EX XD	MO XD
104.00	-20.772	-20.772
112.00	-15.304	-15.252
120.00	-8.945	-8.642
128.00	5.235	1.761
136.00	14.533	17.519
144.00	18.268	26.336
152.00	21.553	31.380
160.00	24.680	33.645
168.00	27.477	33.394
176.00	30.123	31.409
184.00	32.009	27.763
192.00	32.151	24.977
200.00	29.383	19.653
208.00	25.357	15.637
216.00	18.734	9.687
224.00	11.733	4.353
232.00	3.148	-1.274
240.00	-4.215	-7.526
248.00	-11.027	-11.564
256.00	-17.658	-13.235
264.00	-31.990	-25.618
272.00	-32.521	-28.772
280.00	-25.254	-22.275
288.00	-21.391	-18.980
296.00	-17.616	-16.833
304.00	-14.795	-13.717
312.00	-10.799	-12.824
320.00	-4.600	-9.903
328.00	0.722	-7.283
336.00	4.382	-1.824
344.00	4.855	0.736
352.00	5.087	2.325
360.00	5.327	3.322
368.00	5.606	4.371
376.00	4.658	4.140
384.00	4.151	4.107
392.00	3.520	3.767
400.00	3.651	3.170

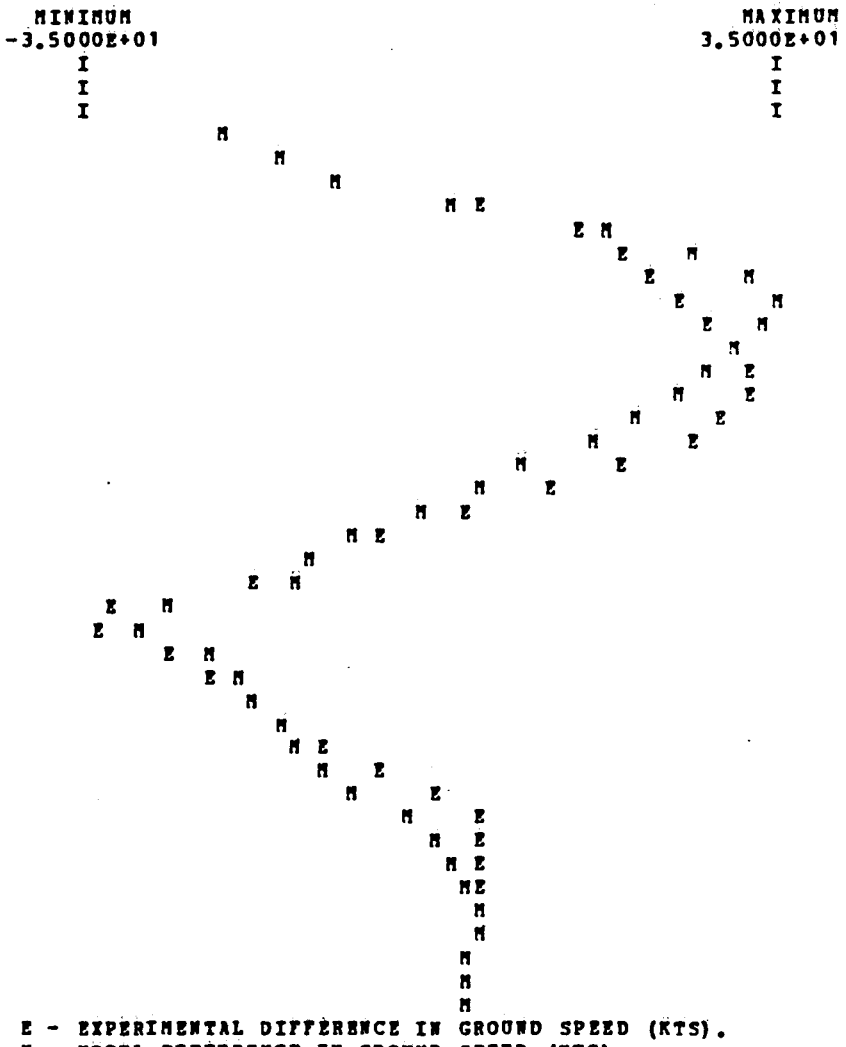

E - EXPERIMENTAL DIFFERENCE IN GROUND SPEED (KTS).
M - MODEL DIFFERENCE IN GROUND SPEED (KTS).

PILOT 2, VCWS, REPLICATION NUMBER 1.
H*=3.45, DELAY=12.0, ZETA = 0.506, OMEGA = 0.0257

b. Velocity data.

Figure 12. - Concluded.

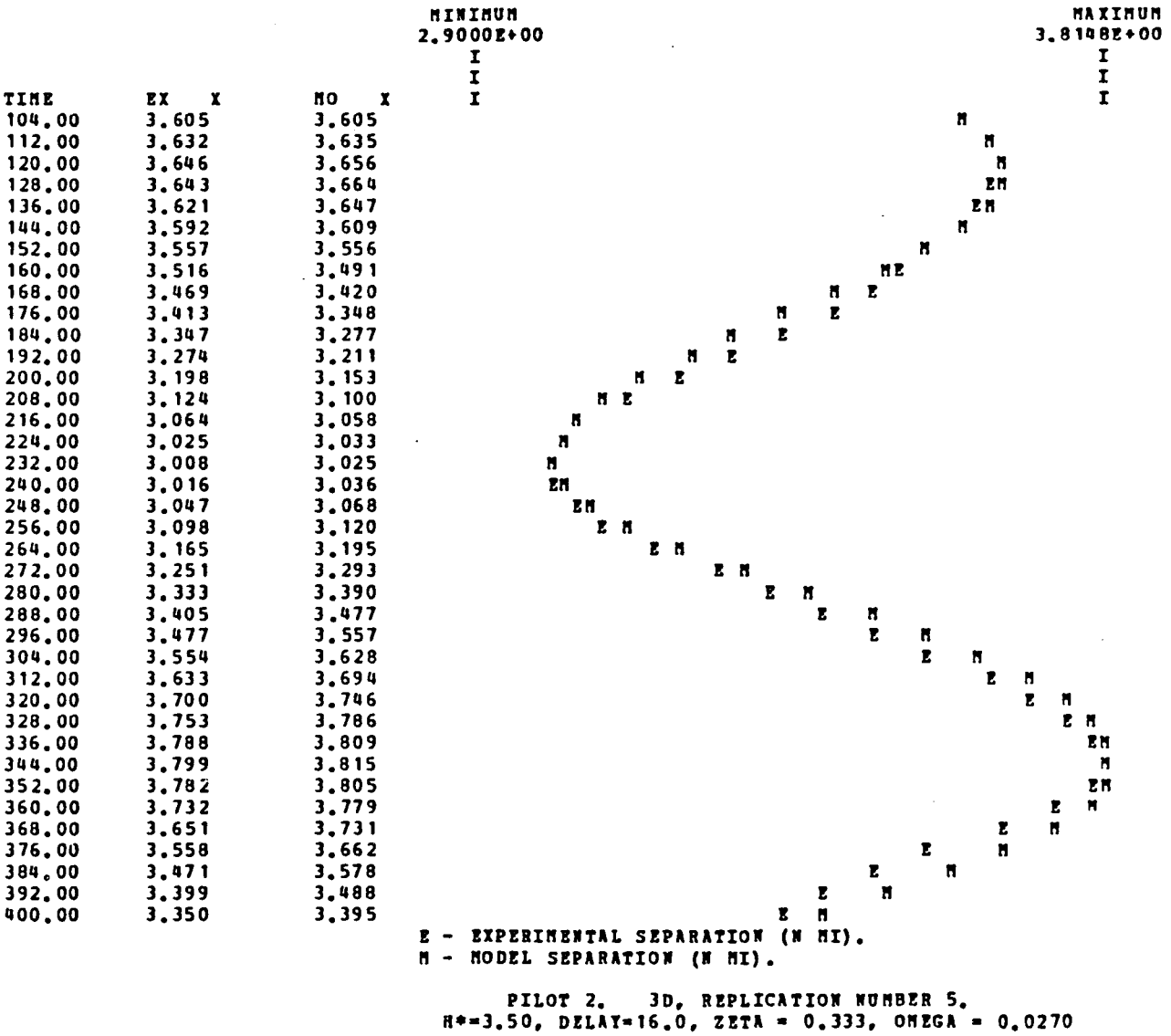

a. Separation data.

Figure 13. - Comparison of experimental and model data.

TIME	EX XD	MO XD
104.00	-15.264	-15.264
112.00	-9.511	-12.245
120.00	-2.853	-7.701
128.00	6.590	1.751
136.00	11.900	12.110
144.00	14.530	20.296
152.00	16.966	26.262
160.00	19.569	30.203
168.00	23.171	31.765
176.00	27.668	31.828
184.00	31.474	30.601
192.00	33.659	27.645
200.00	34.486	23.766
208.00	31.059	21.554
216.00	22.358	14.965
224.00	12.766	7.146
232.00	2.207	-1.576
240.00	-9.134	-10.036
248.00	-18.923	-19.313
256.00	-25.822	-28.093
264.00	-36.098	-40.683
272.00	-39.112	-45.578
280.00	-33.917	-41.892
288.00	-32.085	-38.064
296.00	-33.492	-34.497
304.00	-35.749	-30.528
312.00	-33.584	-27.975
320.00	-27.267	-21.084
328.00	-20.006	-13.944
336.00	-11.177	-8.160
344.00	1.165	0.792
352.00	14.060	6.326
360.00	30.421	16.199
368.00	40.976	26.689
376.00	41.662	35.012
384.00	35.999	38.591
392.00	29.258	42.146
400.00	15.548	41.384

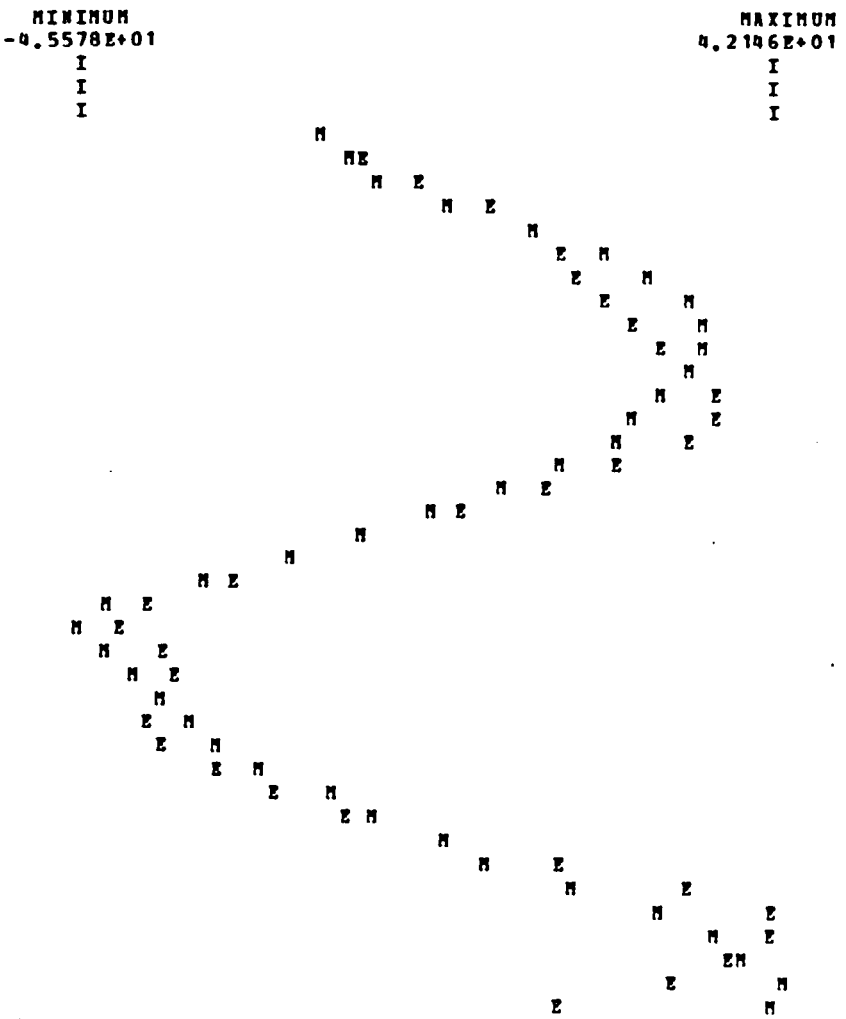

E - EXPERIMENTAL DIFFERENCE IN GROUND SPEED (KTS).
M - MODEL DIFFERENCE IN GROUND SPEED (KTS).

PILOT 2. 3D, REPLICATION NUMBER 5.
H*=3.50, DELAY=16.0, ZETA = 0.333, OMEGA = 0.0270

b. Velocity data.

Figure 13. - Concluded.

TIME	EX X	MO X
104.00	2.981	2.981
112.00	2.974	2.974
120.00	2.967	2.969
128.00	2.958	2.966
136.00	2.940	2.956
144.00	2.921	2.939
152.00	2.911	2.919
160.00	2.917	2.901
168.00	2.938	2.888
176.00	2.975	2.879
184.00	3.025	2.880
192.00	3.076	2.890
200.00	3.118	2.903
208.00	3.145	2.915
216.00	3.155	2.925
224.00	3.149	2.933
232.00	3.126	2.938
240.00	3.093	2.938
248.00	3.055	2.937
256.00	3.015	2.935
264.00	2.983	2.939
272.00	2.966	2.954
280.00	2.946	2.959
288.00	2.923	2.956
296.00	2.907	2.957
304.00	2.891	2.966
312.00	2.870	2.973
320.00	2.846	2.981
328.00	2.818	2.985
336.00	2.796	2.985
344.00	2.786	2.986
352.00	2.786	2.987
360.00	2.797	2.992
368.00	2.811	2.997
376.00	2.828	3.001
384.00	2.847	3.006
392.00	2.864	3.009
400.00	2.879	3.010

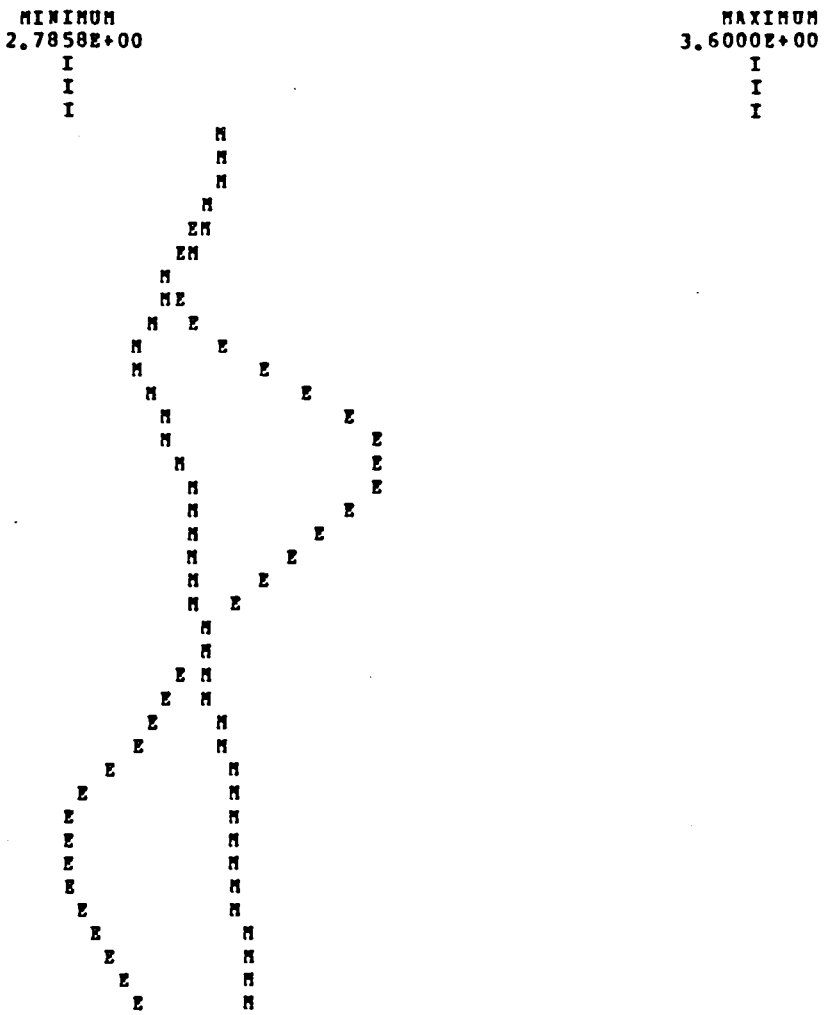

E - EXPERIMENTAL SEPARATION (N MI).
M - MODEL SEPARATION (N MI).

PILOT 1. VCWS, REPLICATION NUMBER 4.
H*=3.00, DELAY= 0.0, ZETA = 0.347, OMEGA = 0.0384

a. Separation data.

Figure 14. - Comparison of experimental and model data.

TIME	EX XD	MO XD
104.00	2.929	2.929
112.00	3.015	1.934
120.00	3.141	0.669
128.00	6.052	2.062
136.00	9.593	6.500
144.00	6.975	7.691
152.00	1.280	8.550
160.00	-6.203	6.487
168.00	-13.046	4.473
176.00	-19.781	2.096
184.00	-23.918	-3.318
192.00	-21.980	-6.227
200.00	-15.678	-6.197
208.00	-8.381	-5.641
216.00	-0.760	-4.551
224.00	6.553	-3.589
232.00	13.584	-0.665
240.00	16.079	-0.592
248.00	18.345	0.739
256.00	17.483	0.522
264.00	9.560	-6.472
272.00	7.462	-5.585
280.00	10.747	0.285
288.00	9.192	0.813
296.00	5.519	-4.213
304.00	8.799	-3.425
312.00	9.870	-4.208
320.00	12.268	-3.624
328.00	12.042	-0.787
336.00	7.248	-0.551
344.00	2.091	-0.995
352.00	-2.652	-1.308
360.00	-5.722	-2.668
368.00	-6.824	-2.269
376.00	-8.235	-2.125
384.00	-8.396	-2.401
392.00	-7.126	-1.309
400.00	-5.577	0.125

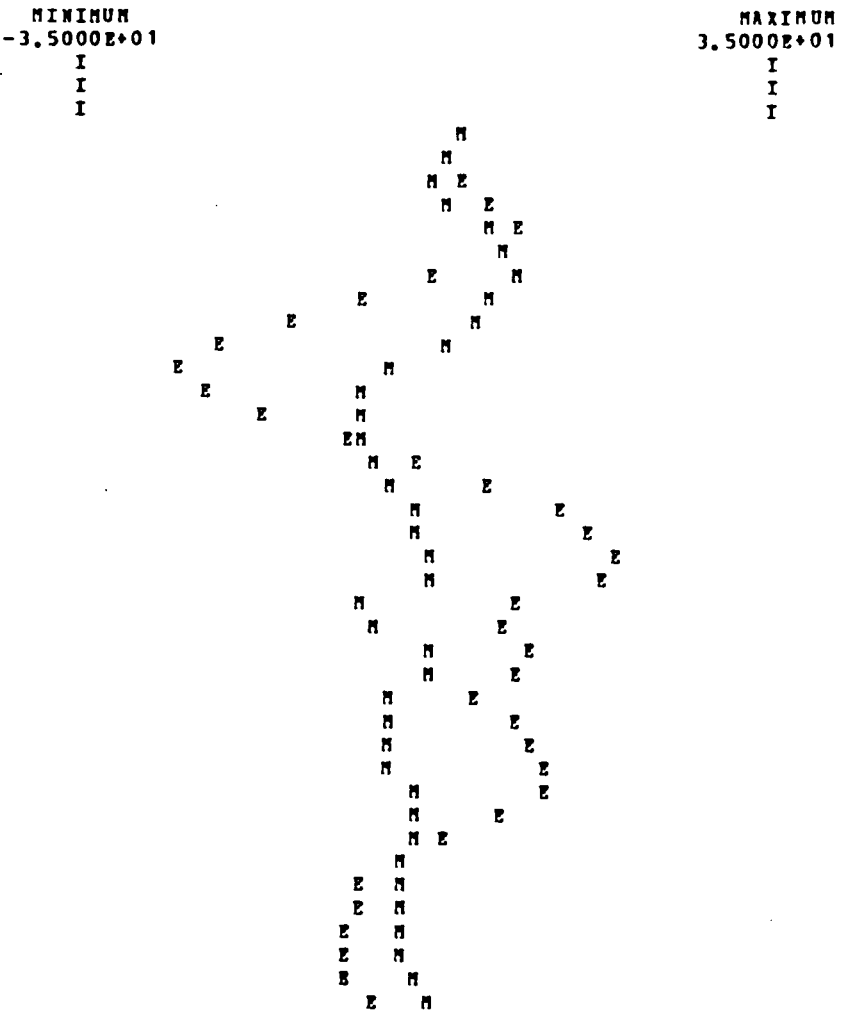

E - EXPERIMENTAL DIFFERENCE IN GROUND SPEED (KTS).
M - MODEL DIFFERENCE IN GROUND SPEED (KTS).

PILOT 1, VCWS, REPLICATION NUMBER 4.
H*=3.00, DELAY= 0.0, ZETA = 0.347, OMEGA = 0.0384

b. Velocity data.

Figure 14. - Concluded

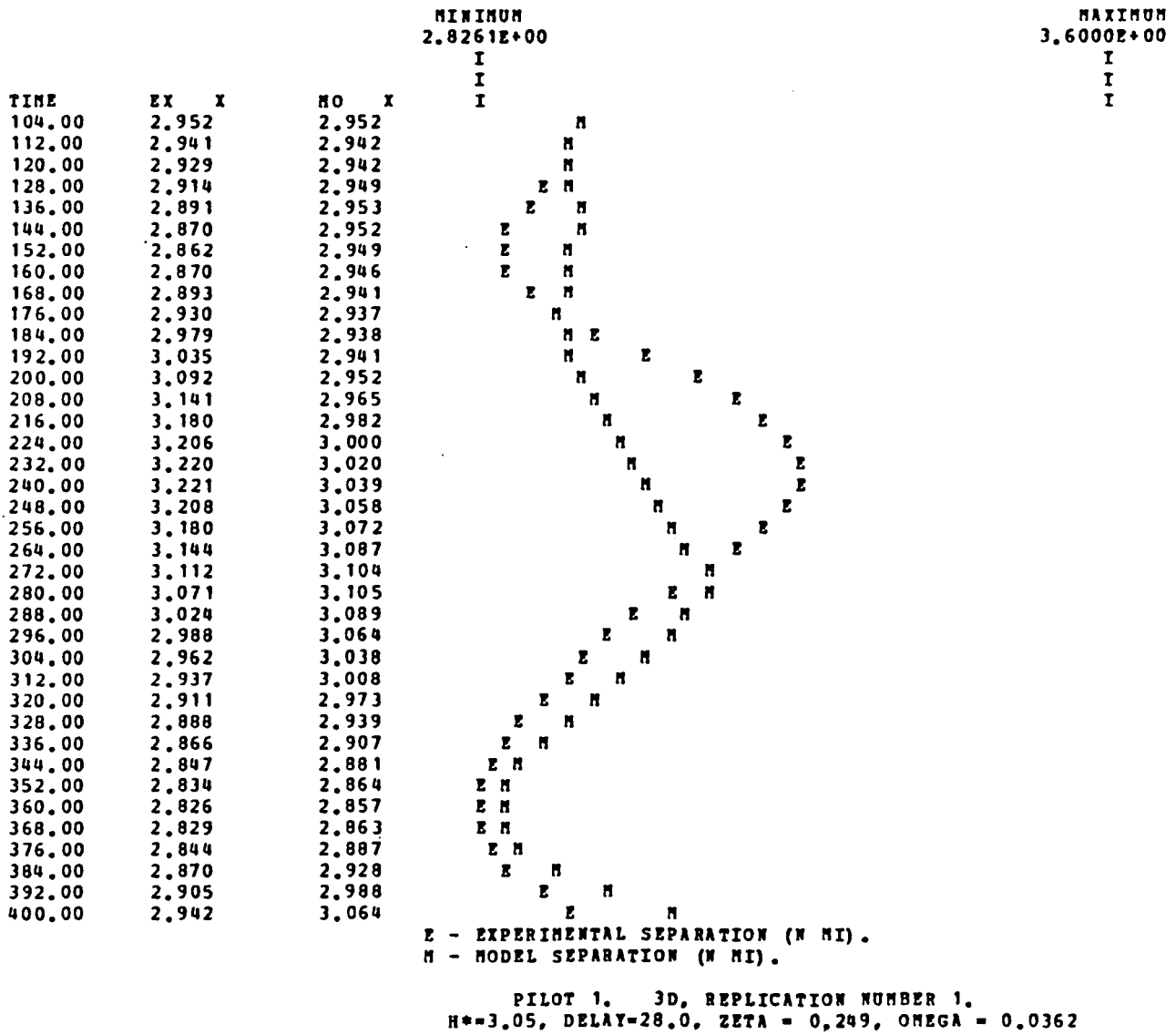

a. Separation data.

Figure 15. - Comparison of experimental and model data.

TIME	EX XD	MO XD
104.00	4.858	4.858
112.00	5.138	1.503
120.00	5.620	-2.332
128.00	8.412	-3.938
136.00	11.219	-0.762
144.00	6.977	0.511
152.00	0.082	1.075
160.00	-6.798	1.513
168.00	-13.639	1.719
176.00	-19.939	-0.055
184.00	-23.305	-0.670
192.00	-26.761	-3.640
200.00	-24.090	-6.083
208.00	-19.867	-7.253
216.00	-14.824	-8.373
224.00	-9.262	-9.174
232.00	-3.130	-9.104
240.00	2.733	-8.966
248.00	9.061	-8.076
256.00	15.660	-6.093
264.00	14.991	-8.508
272.00	15.623	-5.673
280.00	20.931	3.544
288.00	19.588	9.714
296.00	12.947	11.013
304.00	11.424	12.239
312.00	11.637	14.391
320.00	11.273	15.393
328.00	10.001	14.215
336.00	9.297	12.788
344.00	7.201	9.760
352.00	5.008	4.701
360.00	1.433	0.432
368.00	-3.951	-6.783
376.00	-9.449	-15.060
384.00	-13.929	-23.114
392.00	-16.336	-31.328
400.00	-16.860	-36.786

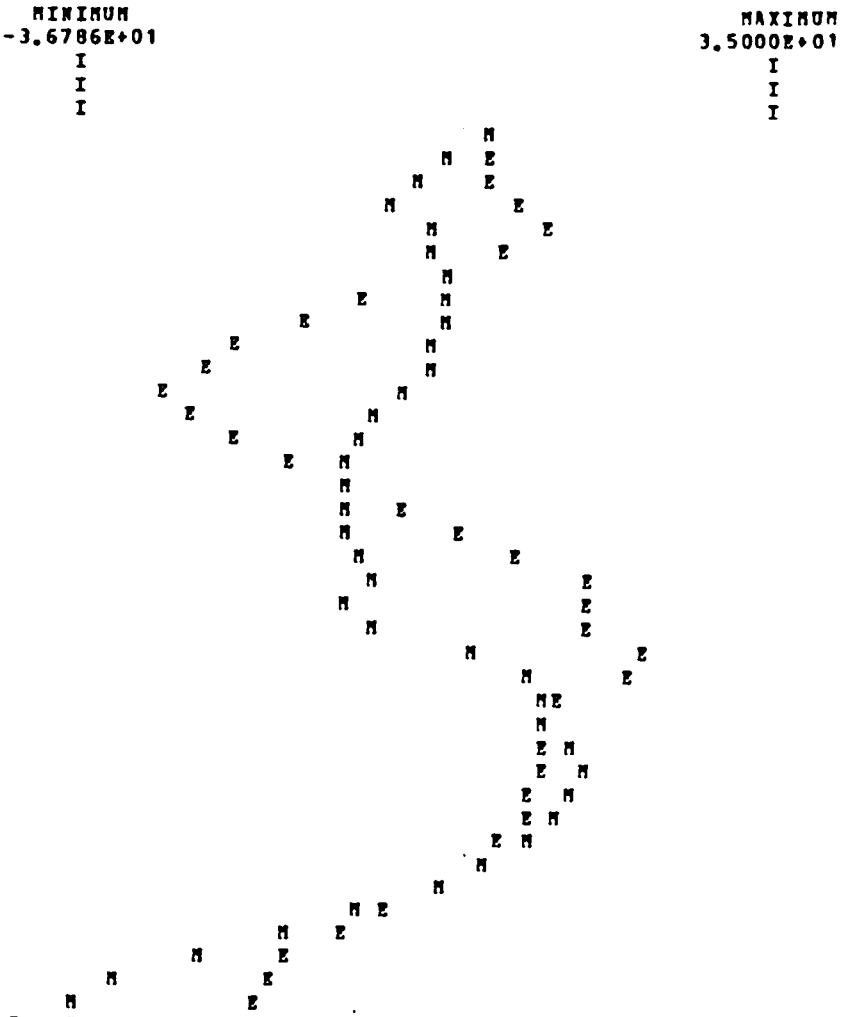

E - EXPERIMENTAL DIFFERENCE IN GROUND SPEED (KTS).
M - MODEL DIFFERENCE IN GROUND SPEED (KTS).

PILOT 1. 3D, REPLICATION NUMBER 1.
H*=3.05, DELAY=28.0, ZETA = 0.249, OMEGA = 0.0362

b. Velocity data.

Figure 15. - Concluded.

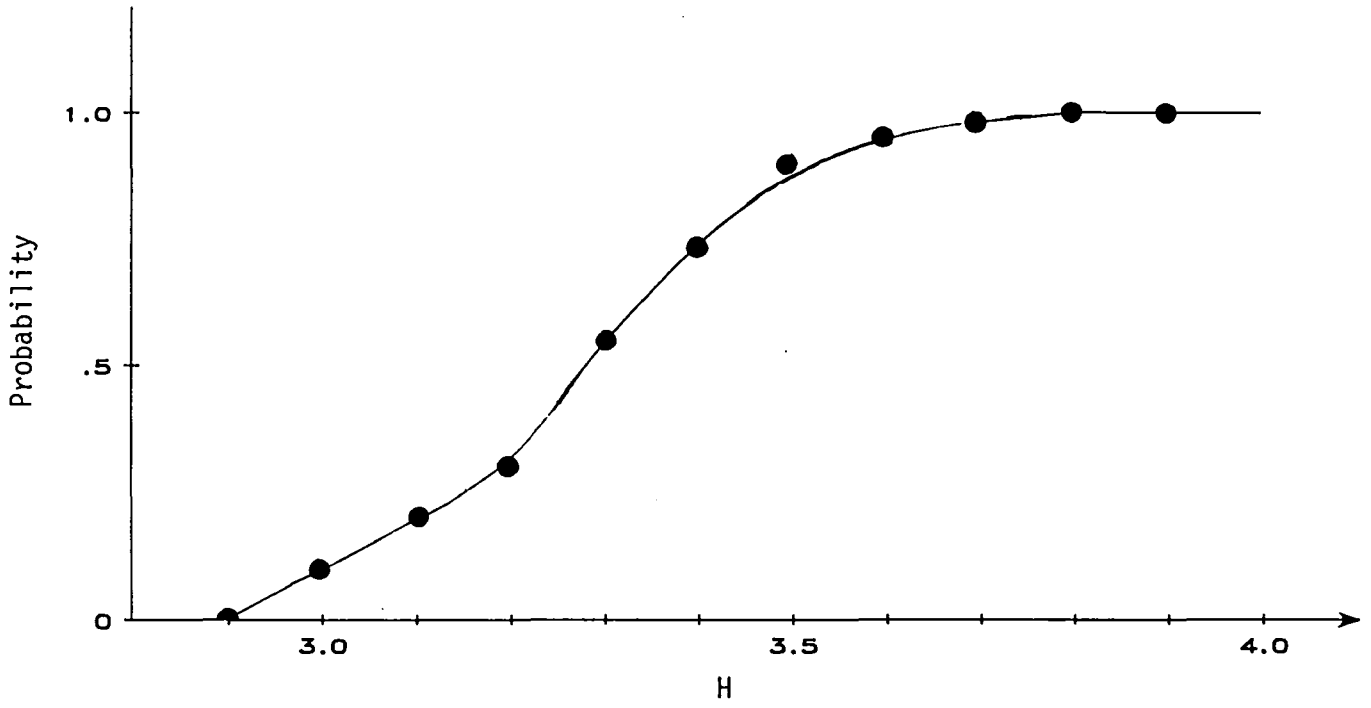

Figure 16. - Cumulative Distribution Function for H.

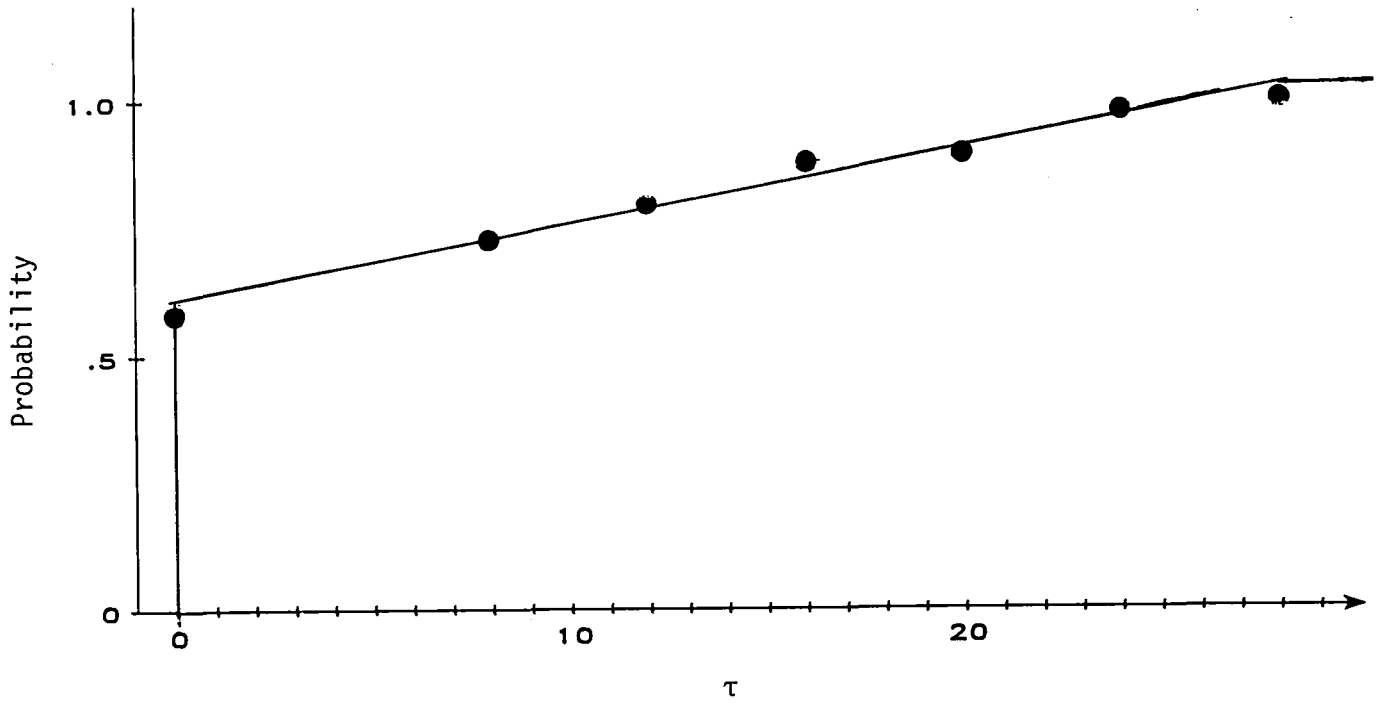

Figure 17. - Cumulative Distribution Function for τ.

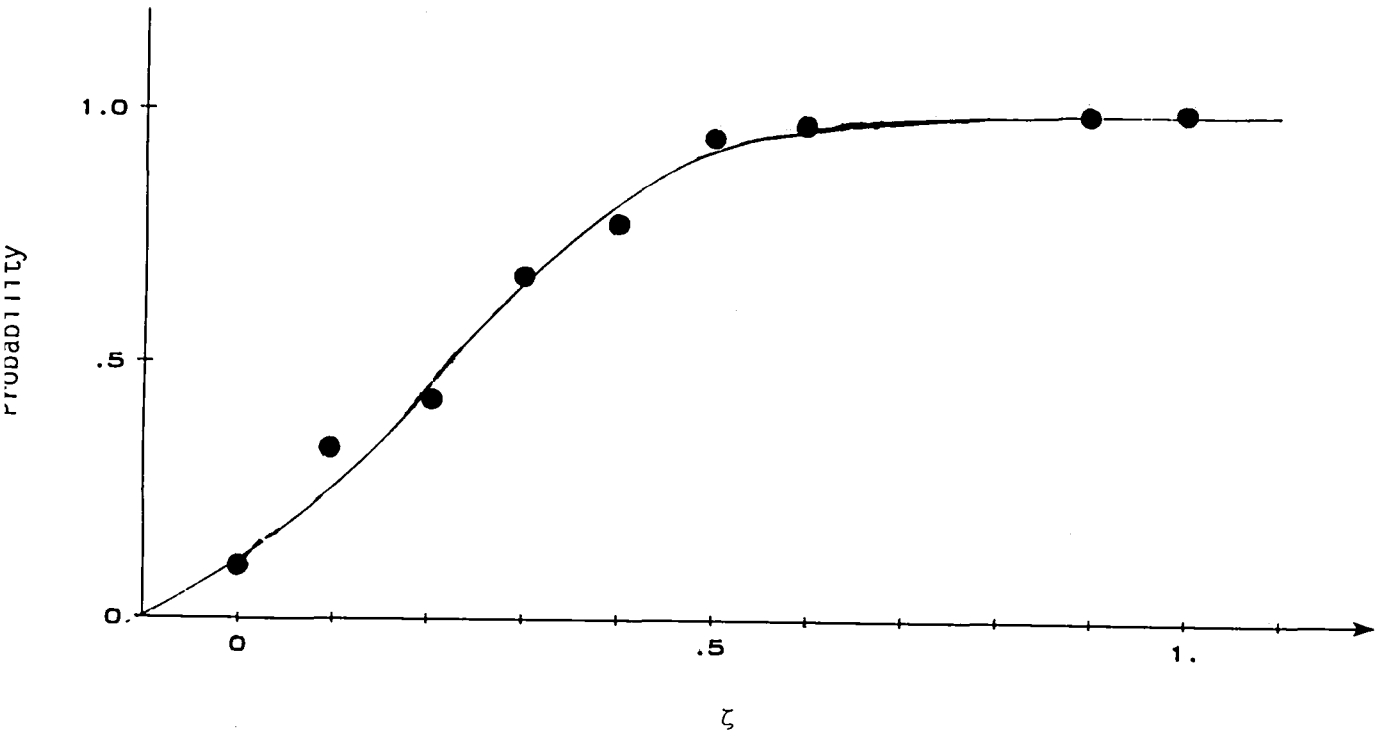

Figure 18. - Cumulative Distribution Function for ζ.

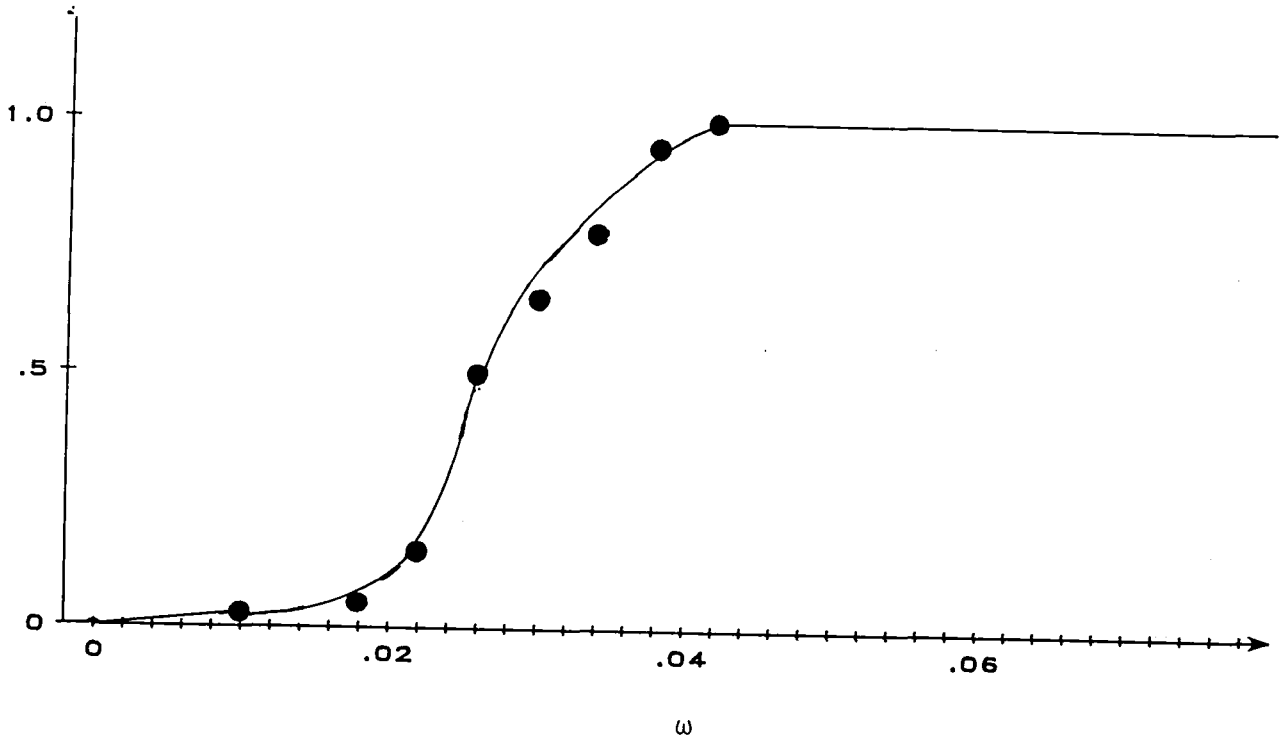

Figure 19. - Cumulative Distribution Function for ω.

1. Report No.	2. Government Accession No.	3. Recipient's Catalog No.
NASA TM-87732		

4. Title and Subtitle	5. Report Date
Development of an Algorithm to Model an Aircraft Equipped with a Generic CDTI Display	July 1986
	6. Performing Organization Code 505-66-41-21

7. Author(s)	8. Performing Organization Report No.
Wade C. Driscoll and Jacob A. Houck	
	10. Work Unit No.
9. Performing Organization Name and Address	
NASA Langley Research Center Hampton, VA 23665-5225	11. Contract or Grant No.
	13. Type of Report and Period Covered Technical Memorandum
12. Sponsoring Agency Name and Address	
National Aeronautics and Space Administration Washington, DC 20546	14. Sponsoring Agency Code

15. Supplementary Notes

Wade C. Driscoll is Professor of Industrial Engineering at Youngstown State University, Youngstown, Ohio and was a participant in the NASA-ASEE Summer Faculty Fellowship Program during 1979 and 1980.

16. Abstract

A model of human pilot performance of a tracking task using a generic Cockpit Display of Traffic Information (CDTI) display is developed from experimental data. The tracking task is to use CDTI in tracking a leading aircraft at a nominal separation of three nautical miles over a prescribed trajectory in space. The analysis of the data resulting from a factorial design of experiments reveals that the tracking task performance depends on the pilot and his experience at performing the task. Performance was not strongly affected by the type of control system used (velocity vector control wheel steering versus 3D automatic flight path guidance and control). The model that is developed and verified results in state trajectories whose difference from the experimental state trajectories is small compared to the variation due to the pilot and experience factors.

17. Key Words (Suggested by Author(s))	18. Distribution Statement
Aircraft Simulation Air Traffic Control	Unclassified - Unlimited Subject Category 59

19. Security Classif. (of this report)	20. Security Classif. (of this page)	21. No. of Pages	22. Price*
Unclassified	Unclassified	57	A04

* For sale by the National Technical Information Service, Springfield, Virginia 22161

End of Document